Physic-guided interpretable data-driven simulations

FEM@LLNL Seminar

November 14, 2023

Youngsoo Choi

LLNL-PRES-854605

This work was performed under the auspices of the U.S. Department of Energy by Lawrence Livermore National Laboratory under contract DE-AC52-07NA27344. Lawrence Livermore National Security, LLC

Lawrence Livermore National Laboratory

Physical simulations play an important role in modern science

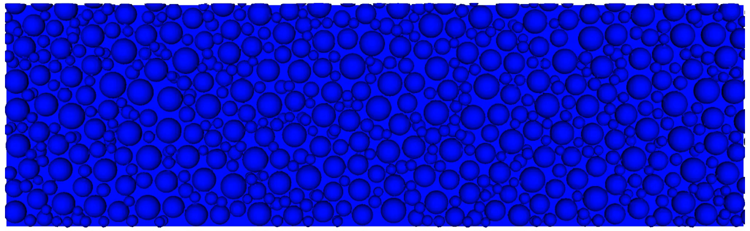

Powder bed fusion AM procedure
(1 week on 108 cores) ALE3D

3D shaped charge
(23 hours on 96 GPUs)
MARBL

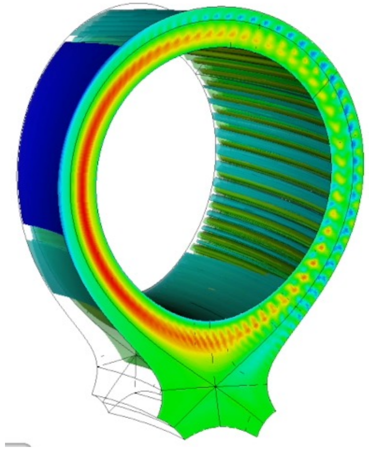

Electrostatic ion-scale turbulence on tokamak fusion device
(5 hours with 1408 cores on NERSC's Cori)
COGENT

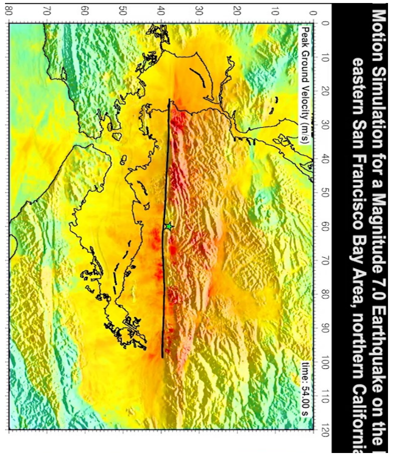

Seismic earthquake
(12 hours on 450,000 cores)
SW4

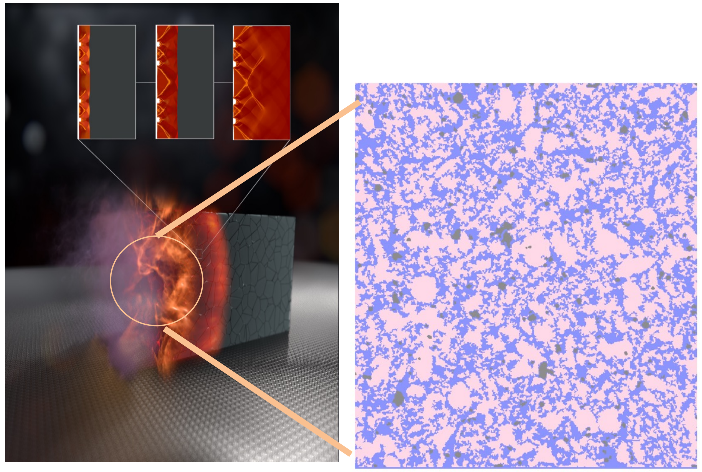

Pore-collapse (1 week on 1024 cores) ALE3D

El Capitan: A high performance computing machine at LLNL

Blackbox

How can you accelerate existing physical simulations? Data

1. Generate Simulation data

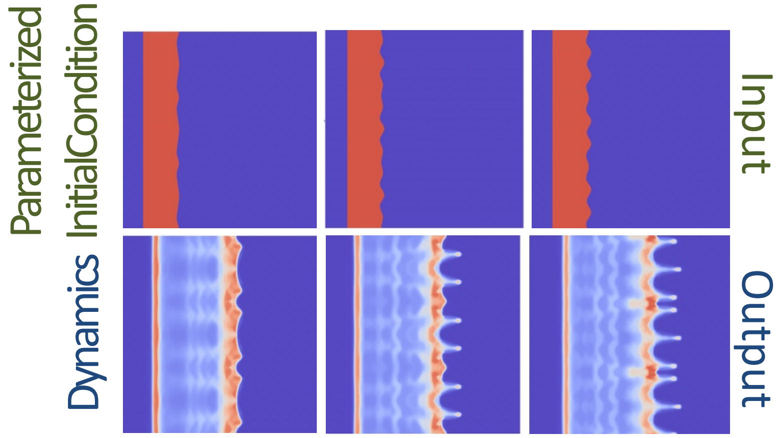

2. Get the relation between input and output,

e.g., training a neural network

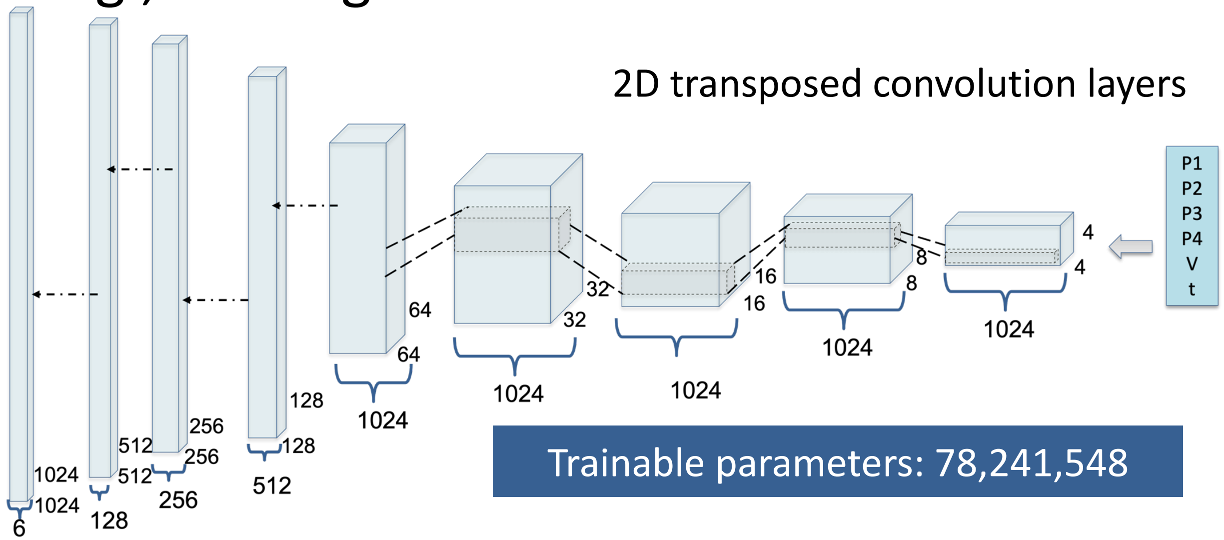

3. Predict

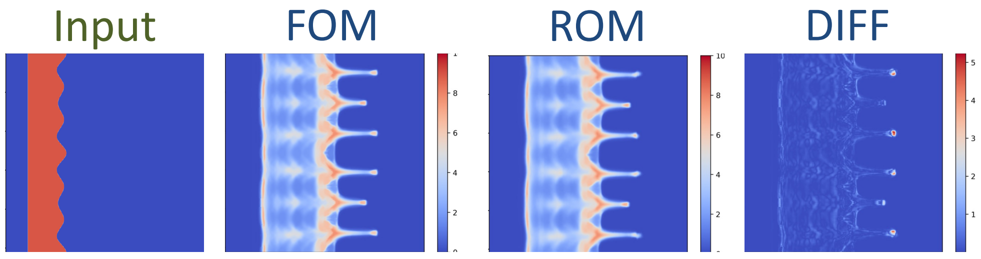

- ☺ Speed-up of 100,000X once trained
- ☺ **Black-box & non-intrusive:** only need data
- ☺ **Less development time** than other data-driven methods
- ☺ Great tools available, e.g., **pyTorch, tensorFlow, …**

Black-box approach has several limitations

16 GB

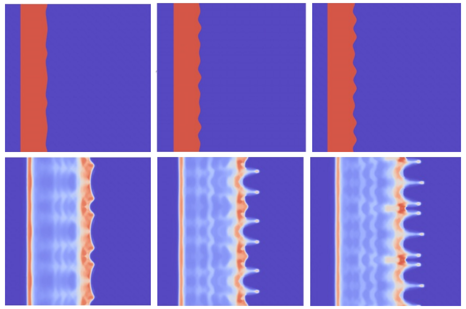

- ☹ Requires **big data → curse of dimensionality**
- ☹ Not easily **interpretable**;
- ☹ Not **structure-preserving**

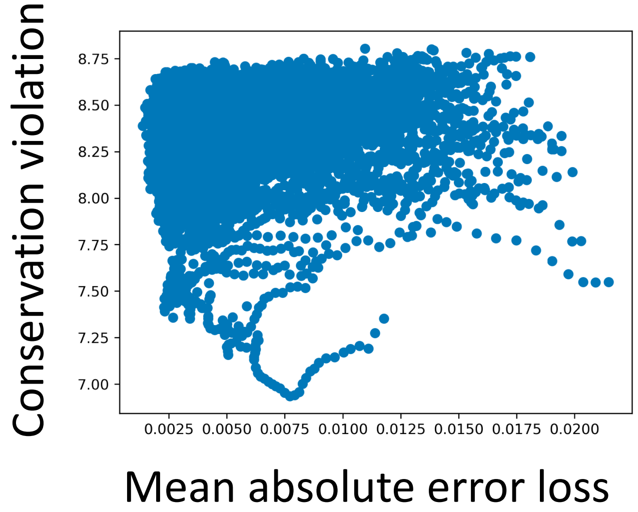

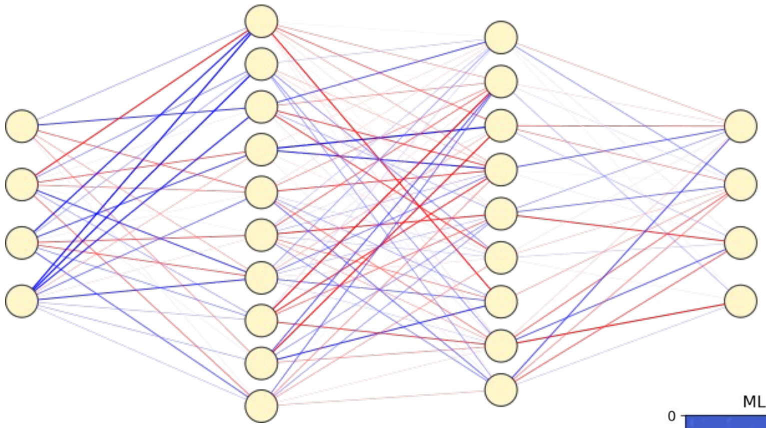

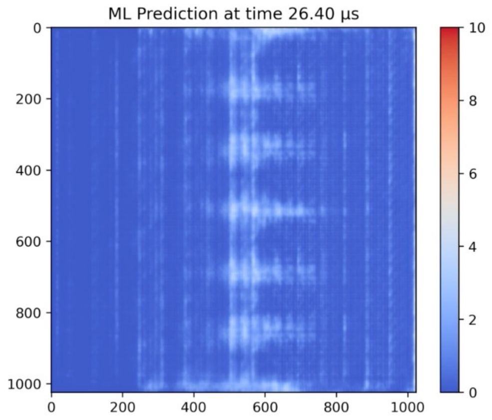

- ☹ Not robust for **extrapolation**

Need: An interpretable and physics-guided data-driven approaches to resolve these issues!

Three goals in reduced order model projects

LaSDI: Latent space dynamics identification

Physics-guided
- Structure-preserving

Interpretable
- Differential equations

Physics discovery
- Identification

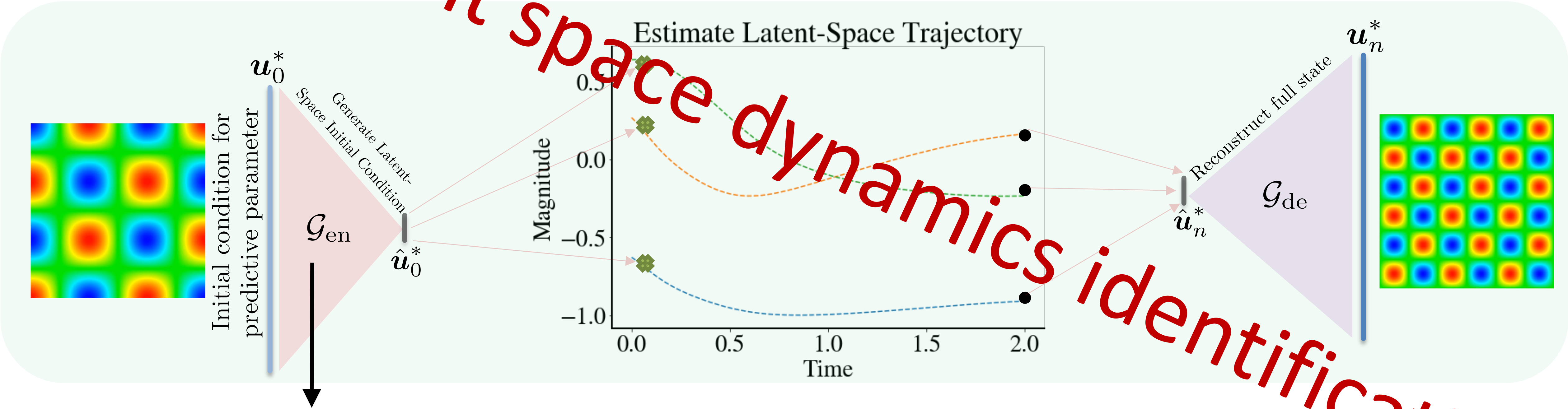

linear compression (e.g., SVD)
nonlinear compression (e.g., AE)

Solve underlying physics governing equations in the reduced space with $\hat{u}(0) = \hat{u}_0^*$

Addressing issue of **requiring big data**

Physics-guided greedy sampling

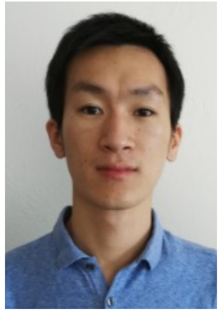
X. He

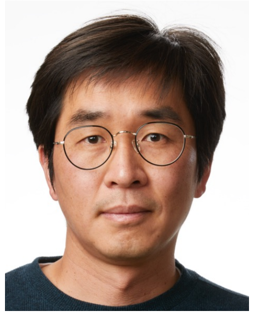
Y. Choi


W. Fries


J. Belof


J.S. Chen

Addressing issue of **space-filling sampling**

Uniform sampling

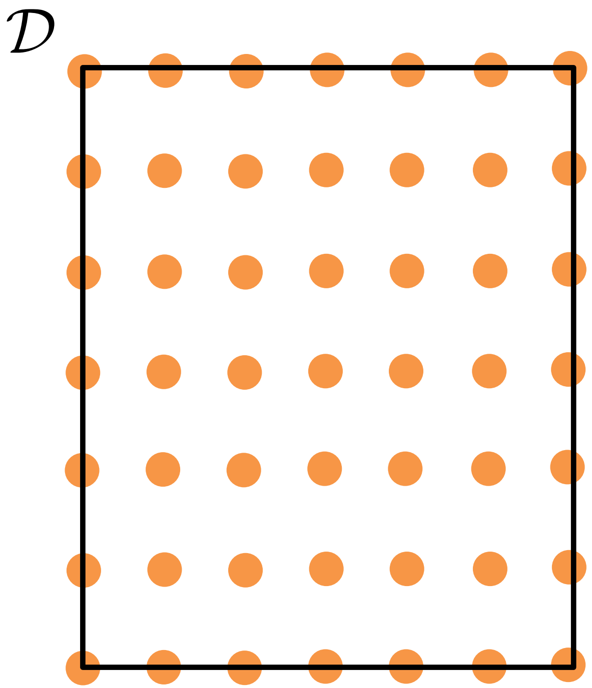

7^2 training points for 1% relative error in 2D

need about **300 million** points in 10D

Optimal sampling

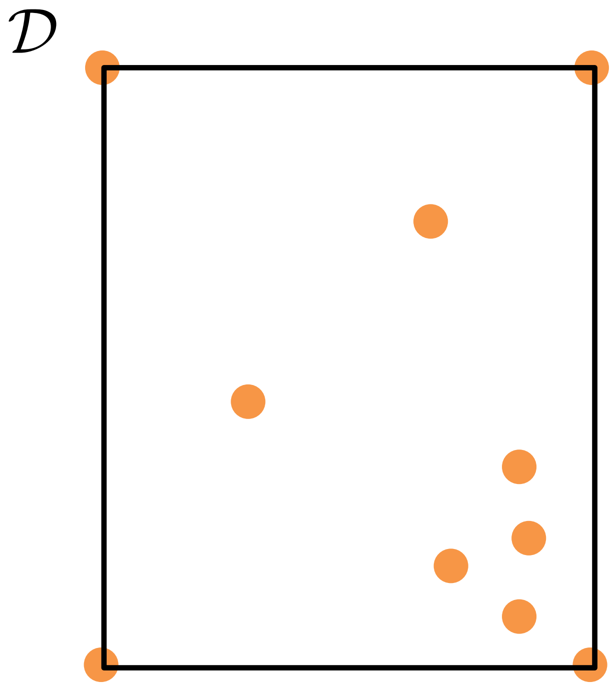

10 training points for 1% relative error in 2D

need about **100 thousand** points in 10D

Physics-informed greedy sampling will help achieving optimal sampling*

A data-driven model training

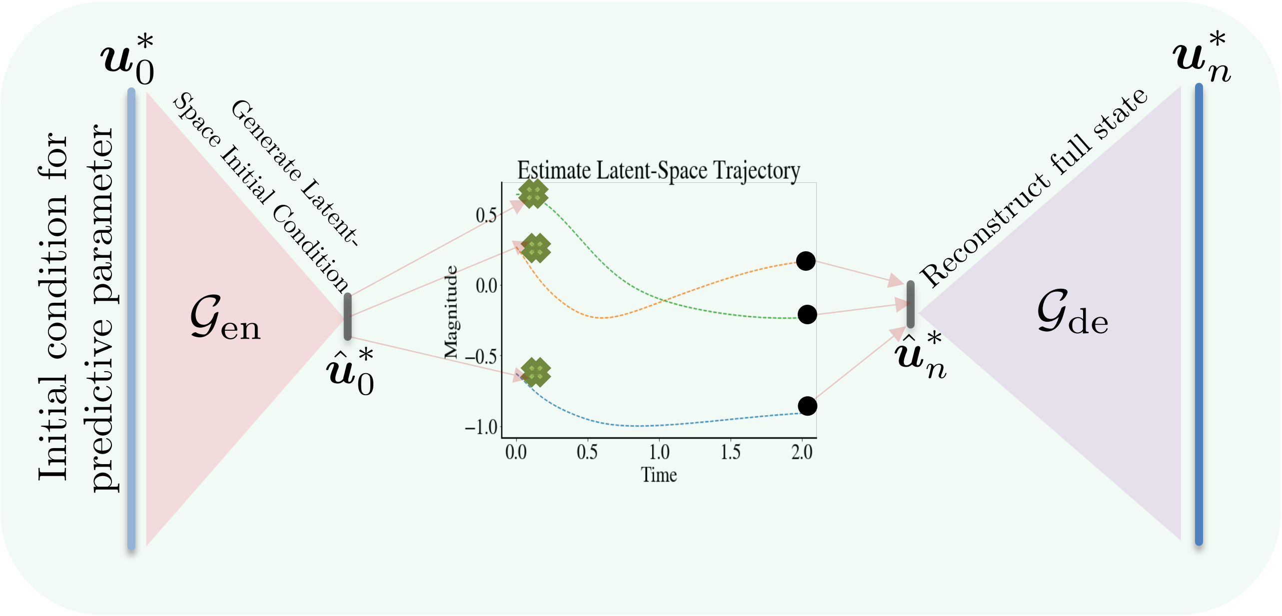

While $N_\mu \leq N_\mu^{max}$:

Model Training

Sampling:

Random Selection

Error Indicator

$N_\mu \leftarrow N_\mu + 1$

End

Greedy Sampling Iteration

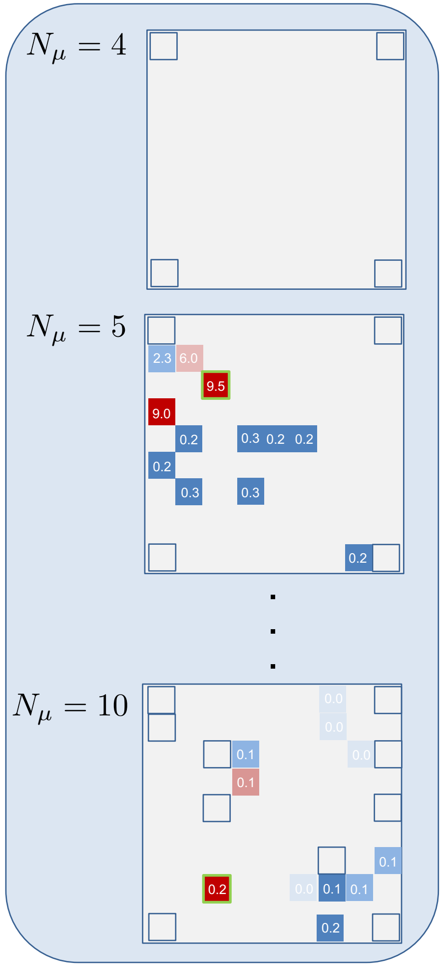

*He, Choi, Fries, Belof, Chen. "gLaSDI: Parametric Physics-informed Greedy Latent Space Dynamics Identification." *JCP*. 2023

Physics-informed sampling reduces the necessary training data

Uniform sampling

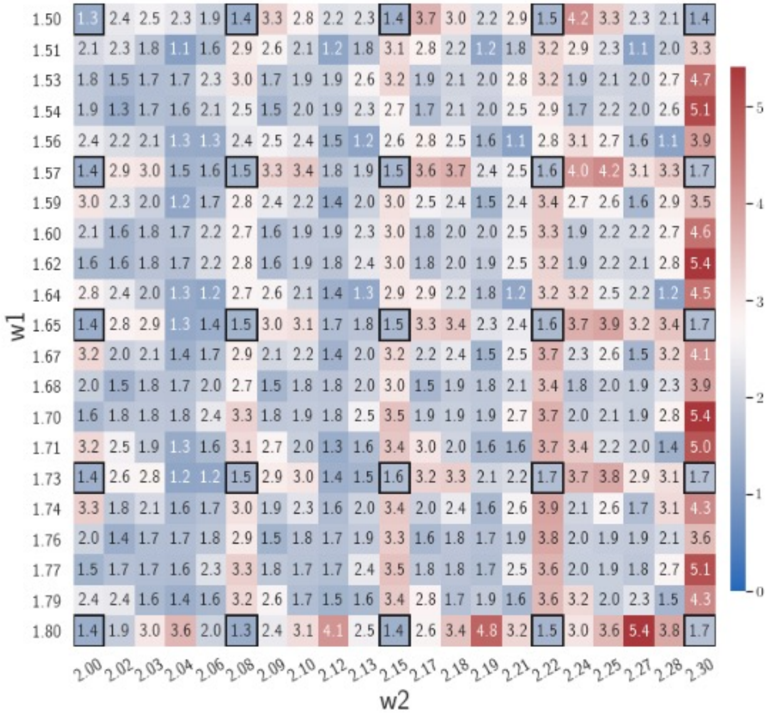

Maximum relative error:

5.4% with 25 uniformly sampled training points

Physics-informed greedy sampling

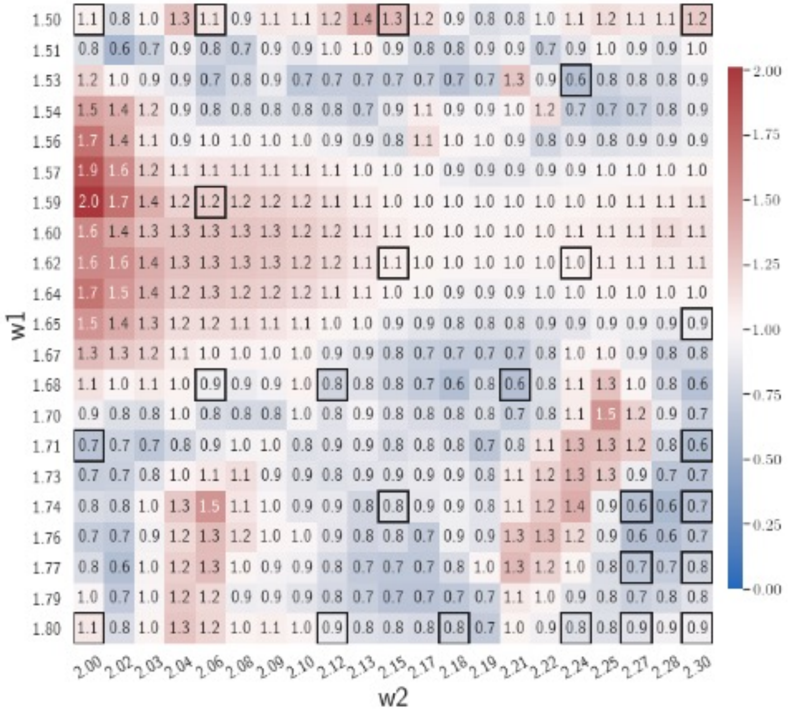

Maximum relative error:

2.0% with 25 greedy sampling points

*He, Choi, Fries, Belof, Chen. "gLaSDI: Parametric Physics-informed Greedy Latent Space Dynamics Identification." *JCP*. 2023

Gaussian process-based sampling

C. Bonneville

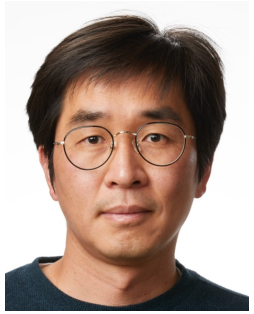

Y. Choi

D. Ghosh

J. Belof

Greedy latent space dynamics identification*

A data-driven model training

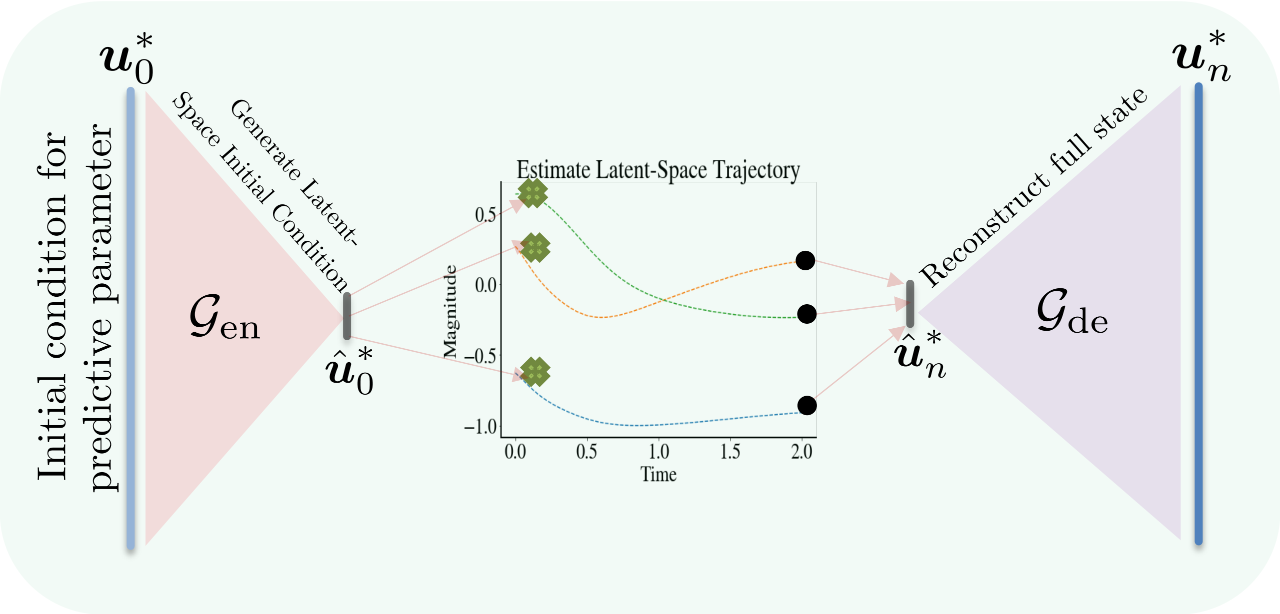

While $m < n_{iter}$:

- Autoencoder training (1)
- If $m \equiv 0 \mod s_r$:
  - GP training (2)
  - For $\xi^* \in \Xi^*$:
    - Find $\max_{(t,x)} \mathbb{V}[\tilde{u}_{\xi^*}]$ (3)
  - End
  - Run FOM for parameter: $\xi_{n+1} = \arg\max_{\xi^*} \left[\max_{(t,x)} \mathbb{V}[\tilde{u}_{\xi^*}]\right]$
- End
- $m = m + 1$

End

Greedy Sampling Iteration

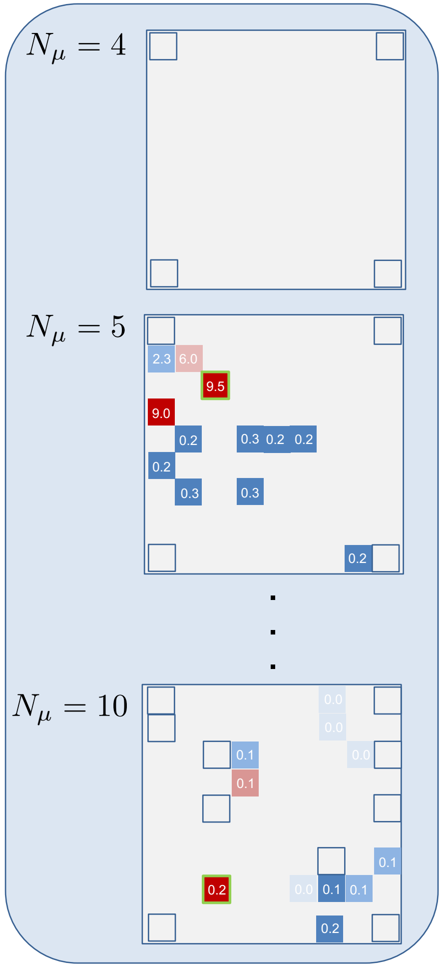

*He, Choi, Fries, Belof, Chen. "gLaSDI: Parametric Physics-informed Greedy Latent Space Dynamics Identification." *JCP*. 2023

GPLaSDI for plasma two stream instability

Greedy sampling

- **1D1V Vlasov Equation:**

$$\begin{cases} \frac{\partial f}{\partial t} + v\frac{\partial f}{\partial x} + \phi \frac{q}{m}\frac{\partial f}{\partial v} = 0 & (t,x,v) \in [0,5] \times [0,2\pi] \times [-7,7] \\ \nabla^2 \phi + \rho = 0 & f(t,x,v=\pm 7) = 0 \end{cases}$$

- **Initial condition:**

$$f(t=0,x,v) = \frac{4}{\pi T}\left[1+\frac{1}{10}\cos(k\pi x)\right]\left[\exp\left(-\frac{(v-2)^2}{2T}\right)+\exp\left(-\frac{(v+2)^2}{2T}\right)\right]$$

- **Parameter:** $\xi = \{T, k\}$, with $T \in [0.9, 1.1]$ and $k \in [1.0, 1.2]$

17 data points

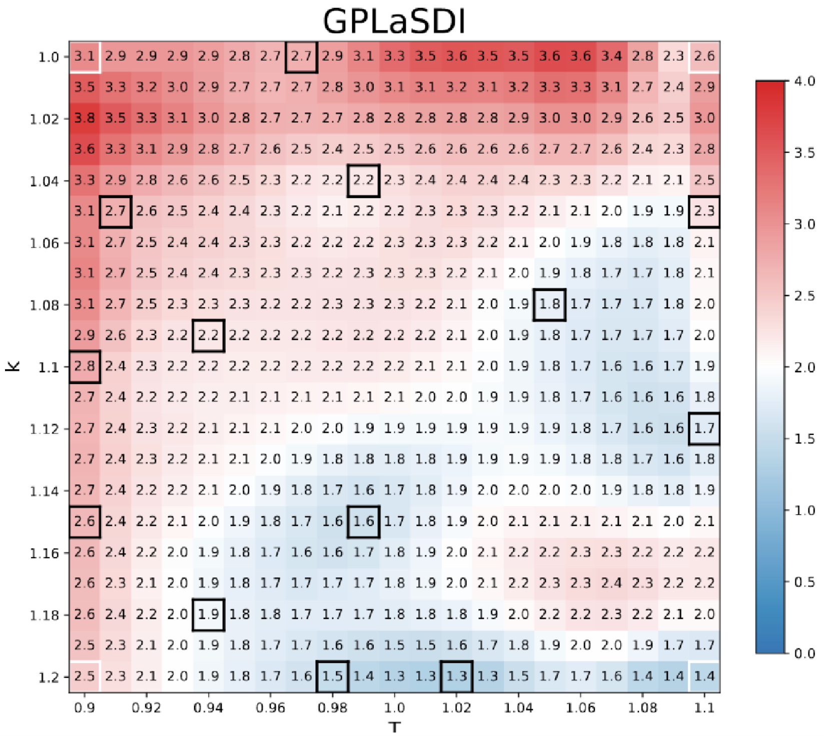

25 data points

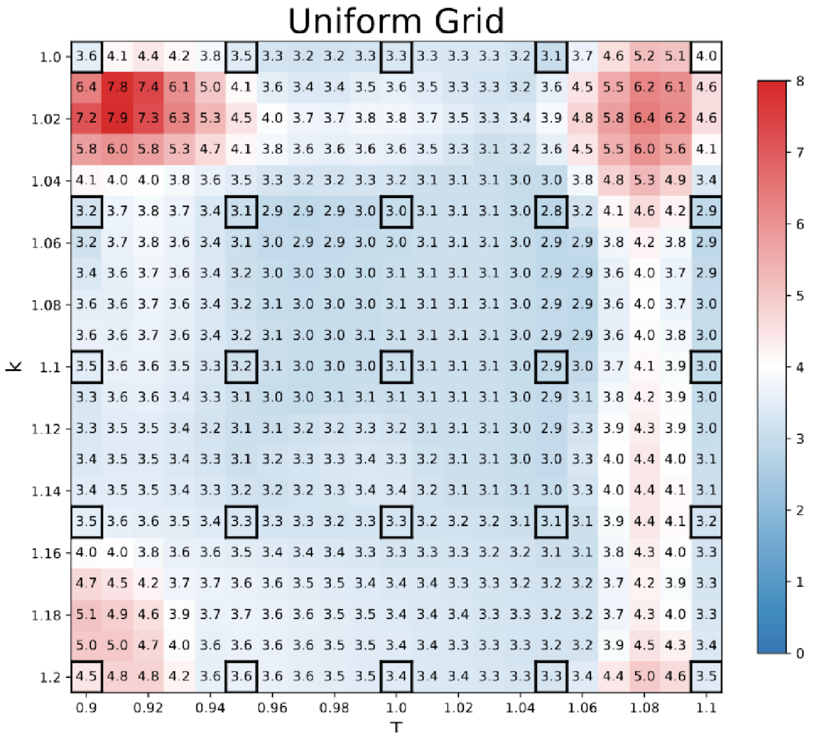

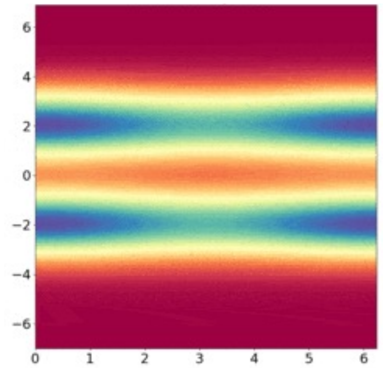

	Run Time (s)	Run Time (s)
FOM	57.9 (1 core)	22.5 (4 cores)
GPLaSDI	0.0118	0.0118
Speed-up	**4906**	**1906**

Addressing issue of **interpretability**

Addressing issue of **interpretability**

Identify **interpretable** governing equations for latent space dynamics

Latent space dynamics data
with dimension of 3

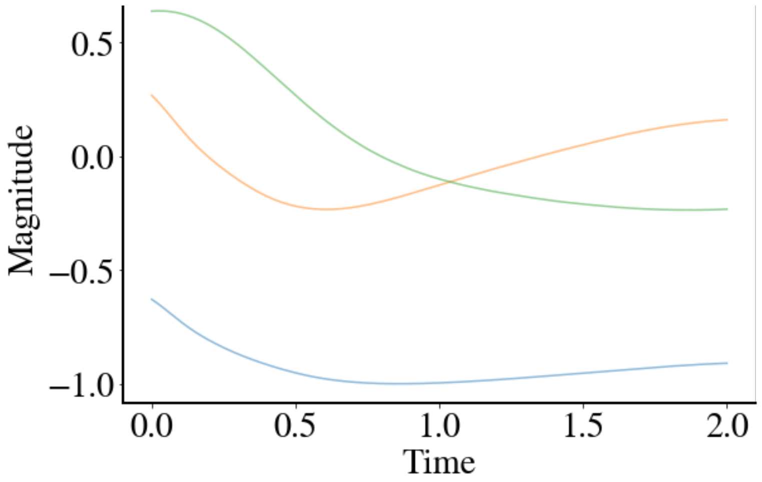

Fit into linear ODE

Dynamic mode decomposition* (DMD):

$$\frac{d\hat{\boldsymbol{u}}}{dt} = \hat{\boldsymbol{A}}(\boldsymbol{\mu})\hat{\boldsymbol{u}}$$

*P.J. Schmid. "Dynamic mode decomposition of numerical and experimental data." Journal of Fluid Mechanics (2010)

Training dynamic mode decomposition

Interpretable

1. Data generation

— Sequence of solution snapshots $\boldsymbol{u}_k = \boldsymbol{u}(t_k)$

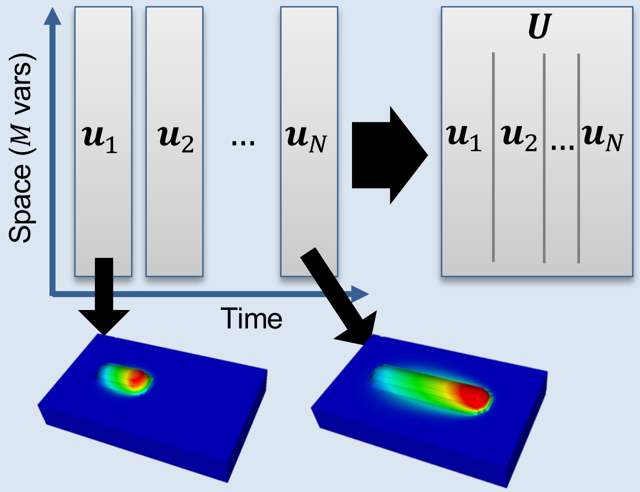

— Define:

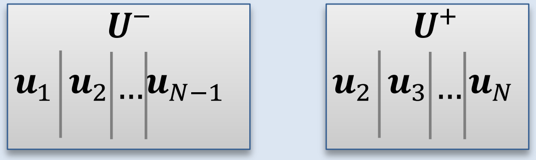

— Find the operator $\boldsymbol{A}$ such that: $\boldsymbol{U}^+ \approx \boldsymbol{A}\boldsymbol{U}^-$

2. Compression

— Singular value decomposition

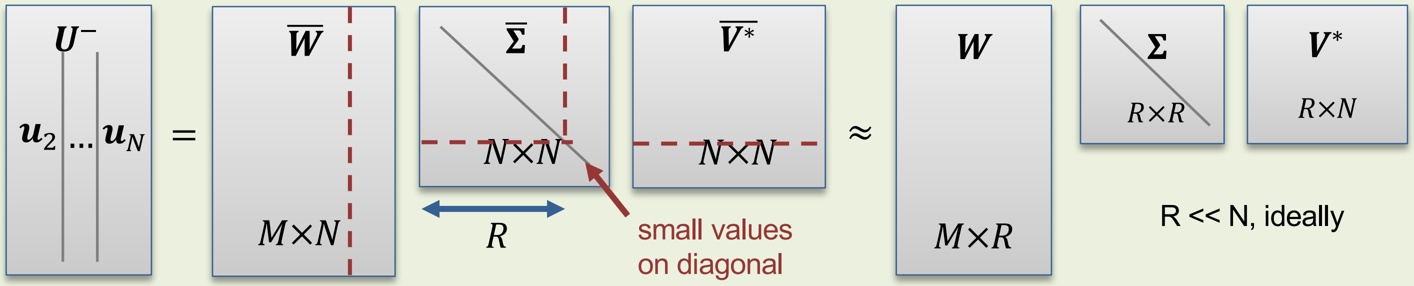

— $\boldsymbol{A} = \boldsymbol{U}^+\boldsymbol{V}\boldsymbol{\Sigma}^{-1}\boldsymbol{W}^*$

— Define reduced matrix (size $R\times R$): $\widetilde{\boldsymbol{A}}_r = \boldsymbol{W}^*\boldsymbol{A}\boldsymbol{W} = \boldsymbol{W}^*\boldsymbol{U}^+\boldsymbol{V}\boldsymbol{\Sigma}^{-1}$

— Reduced space dynamics: $\widetilde{\boldsymbol{u}}_{k+1} = \widetilde{\boldsymbol{A}}_r\widetilde{\boldsymbol{u}}_k$

- $\widetilde{\boldsymbol{u}}_k = \boldsymbol{W}^*\boldsymbol{u}_k$

3. Prediction

— Eigen-decomposition of reduced space

$$\widetilde{\boldsymbol{A}}_r\boldsymbol{X} = \boldsymbol{\Lambda}\boldsymbol{X}$$

— DMD solution at time t:

$$\boldsymbol{u}(t) = \boldsymbol{\Phi}\boldsymbol{\Lambda}^{\frac{t-t_1}{\Delta t}}\boldsymbol{\Phi}^{\dagger}\boldsymbol{u}_1 = \boldsymbol{\Phi}\boldsymbol{\Lambda}^{\frac{t-t_1}{\Delta t}}\boldsymbol{b}_0$$

- where $\boldsymbol{\Phi} = \boldsymbol{W}\boldsymbol{X}$ or $\boldsymbol{\Phi} = \boldsymbol{W}\widetilde{\boldsymbol{A}}_r\boldsymbol{X}$
  $\boldsymbol{b}_0 = \boldsymbol{\Phi}^{\dagger}\boldsymbol{u}_1$

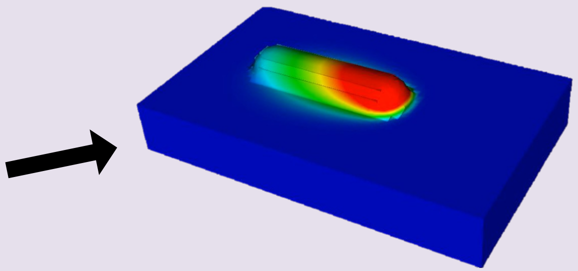

Time/distance windowing DMD

- *Offline phase*
  - Classify data
  - Collect data
  - Compress data
  - Build local DMD
- *Online phase*
  - Assign local DMD
  - Evaluate DMD solution

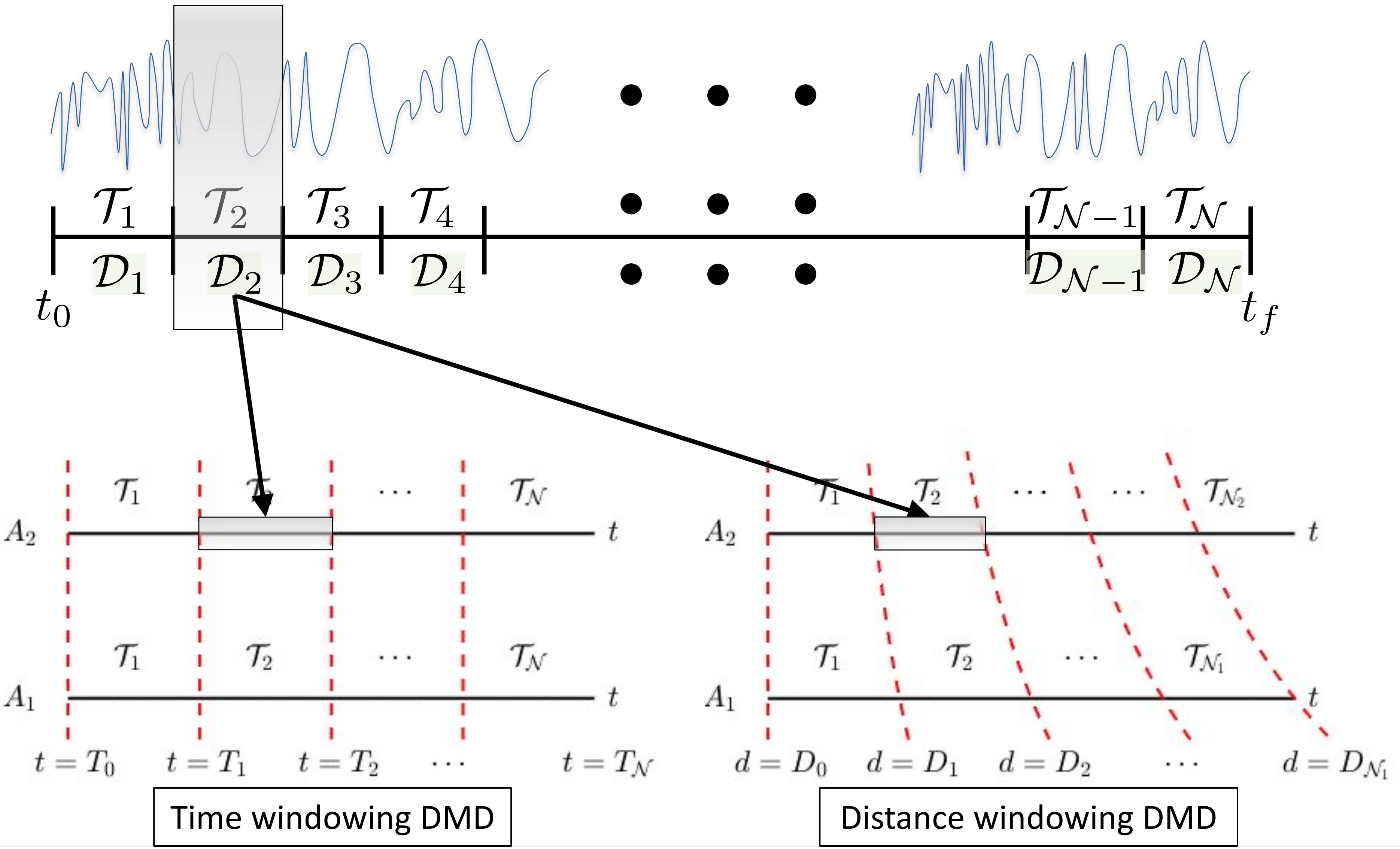

3D printing process DMD


E. Chin


S.W. Cheung

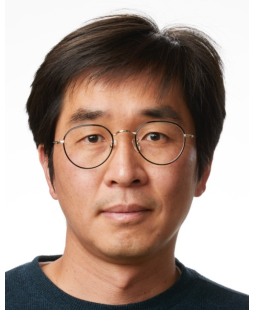
Y. Choi


D. Copeland


S. Khairallah


J. McKeown

Interpretable

Laser powder bed fusion

High-fidelity heating through laser ray-tracing

Full-order model	20% basis truncation	60% basis truncation
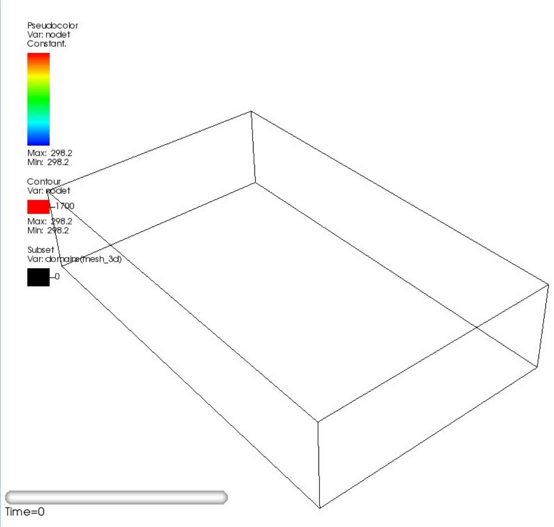	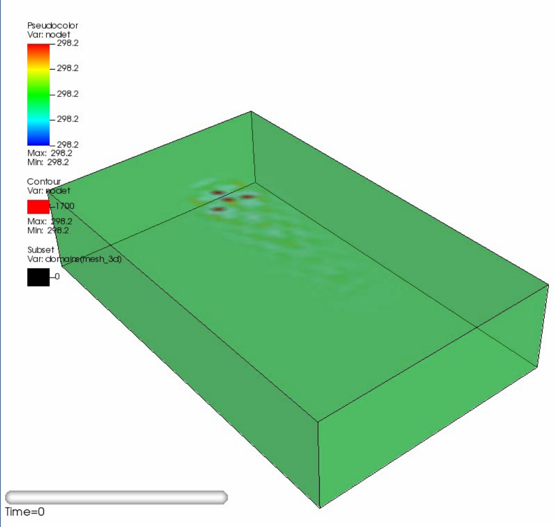	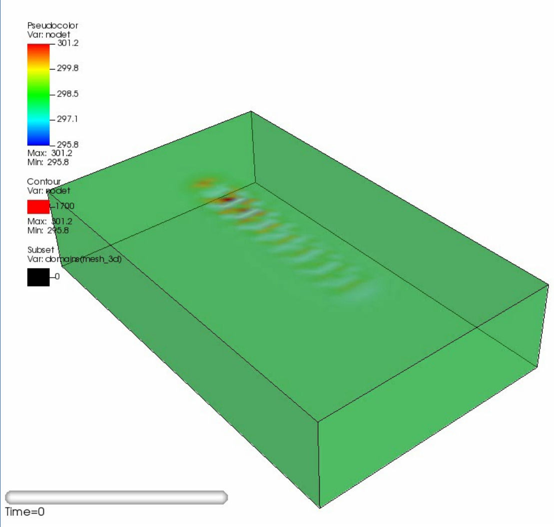
• 100 µs thermal simulation in ALE3D • ~25k DOFs • ~1 hr analysis time	• 0.1% max relative error • 1.65 s prediction time • ~2,000x speedup	• 0.5% max relative error • 0.42 s prediction time • ~8,500x speedup

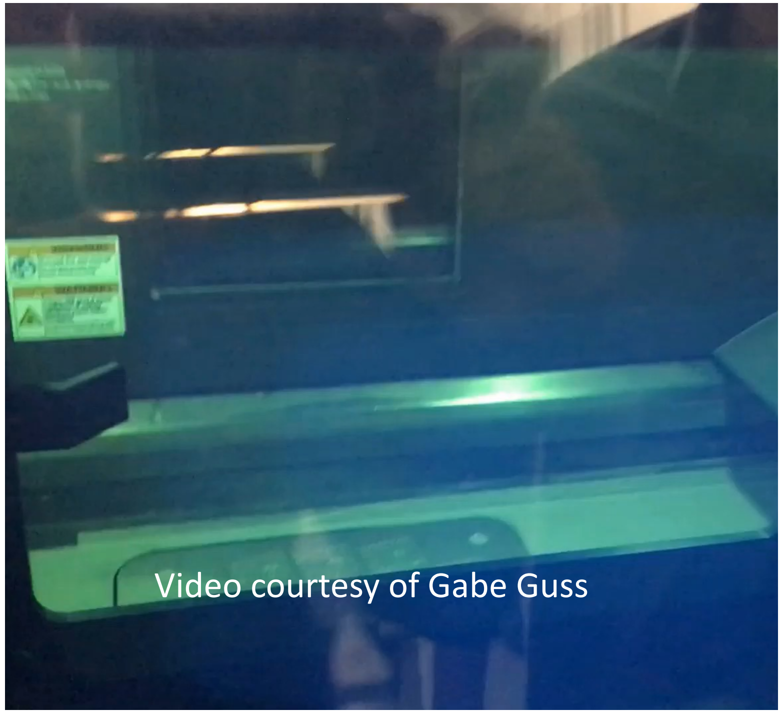

Direct energy deposition

160 Watt laser power, 0.1 m/s scan speed

Full-order model	20% basis truncation	60% basis truncation
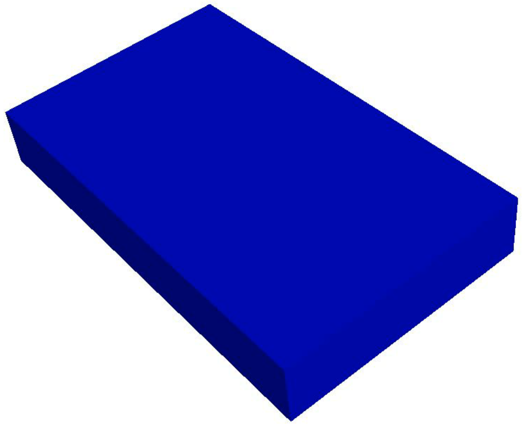	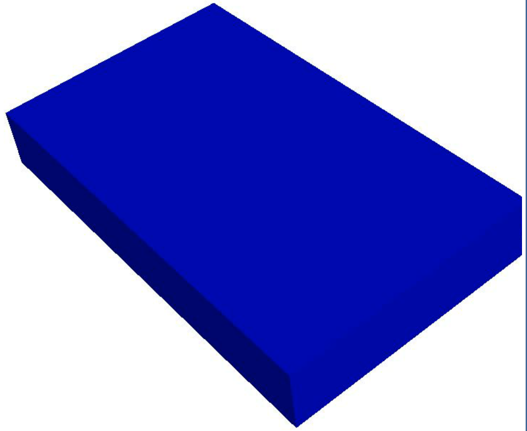	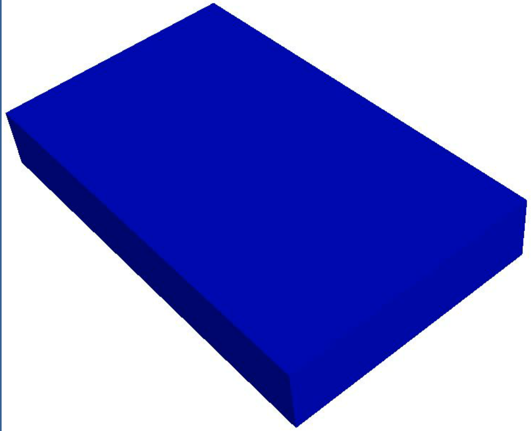
• 25,000 μs thermal simulation in ALE3D • ~25k DOFs • ~0.6 hr analysis time	• 1.6% max relative error • 0.13 s prediction time • ~15,000x speedup	• 2.1% max relative error • 0.03 s prediction time • ~75,000x speedup

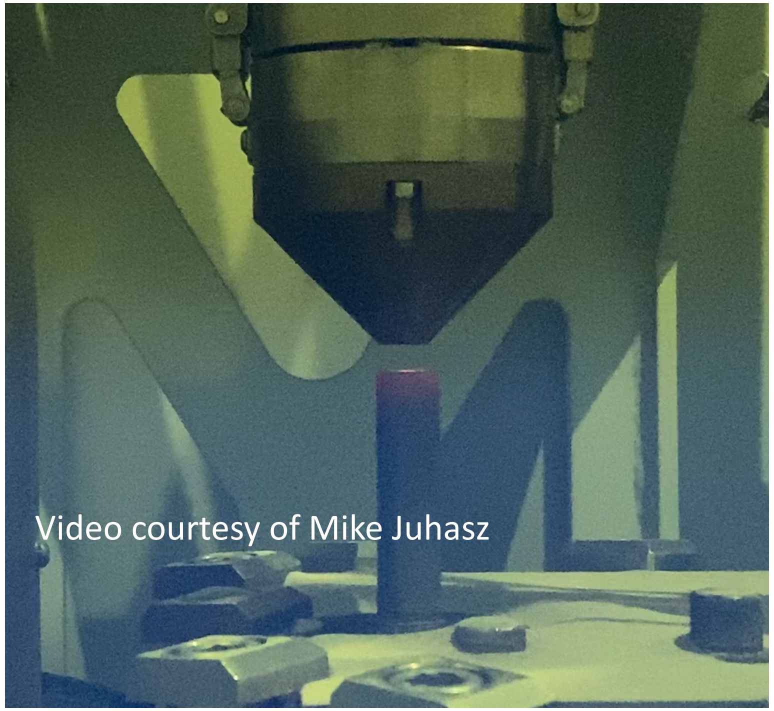

LaSDI: Latent space dynamics identification

W. Fries

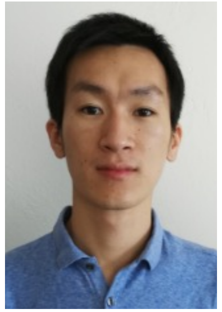

X. He

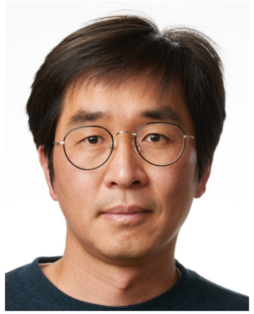

Y. Choi

SINDy* can be used as Latent Space Dynamics Identification (LaSDI)

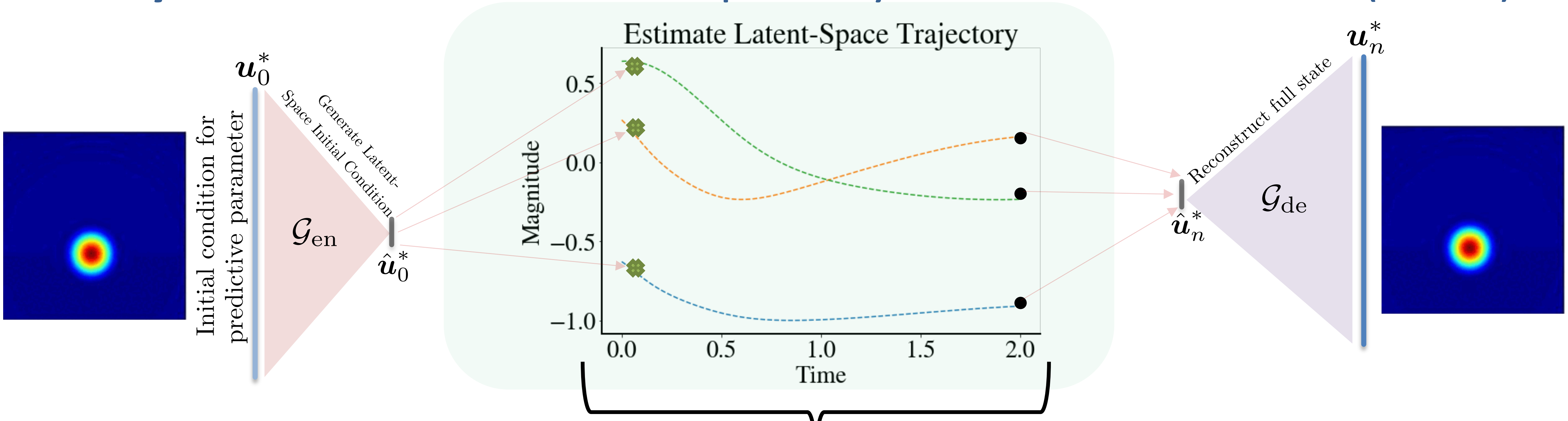

Strong form → $\frac{d\hat{\mathbf{u}}}{dt} = \hat{\mathbf{A}}(\boldsymbol{\mu})\Theta(\hat{\mathbf{u}})$

☹ Not robust for **noisy data**

$$\Theta\left(\hat{U}_k^T\right) = \left[1 \quad \hat{U}_k^T \quad \hat{U}_{k,P_2}^T \quad \ldots \quad \hat{U}_{k,P_\ell}^T \quad \ldots \quad \sin(\hat{U}_k^T) \quad \cos(\hat{U}_k^T) \quad \ldots \quad \exp(\hat{U}_k^T)\right]$$

*Brunton, Steven L., Joshua L. Proctor, and J. Nathan Kutz. "Discovering governing equations from data by sparse identification of nonlinear dynamical systems." Proceedings of the national academy of sciences (2016)

WgLaSDI: Weak greedy LaSDI


A. Tran

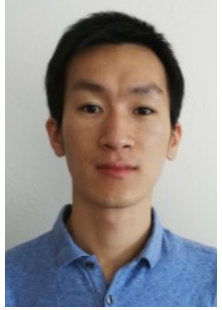
X. He


D. Messenger

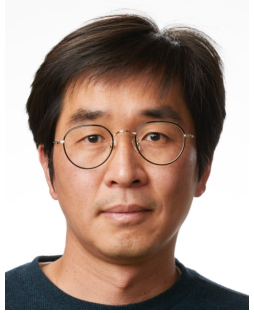
Y. Choi


D. Bortz

wLaSDI: Weak SINDy* in LaSDI for robustness with noisy data

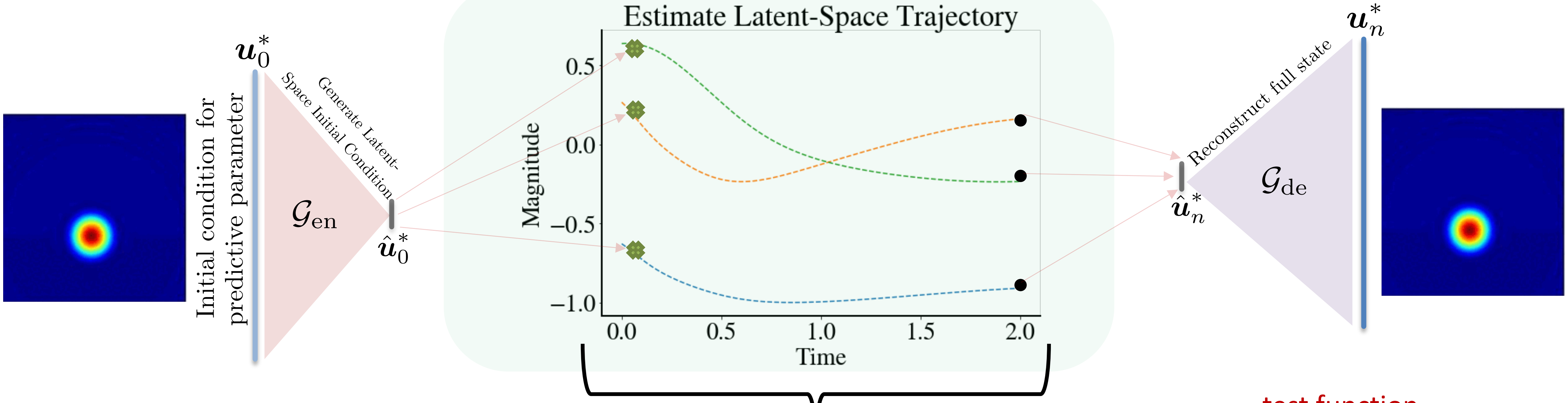

Integration by parts will give Weak form

$$\int_a^b \frac{d\hat{\mathbf{u}}}{dt}\phi(t)dt = \int_a^b \hat{\boldsymbol{A}}(\boldsymbol{\mu})\Theta(\hat{\boldsymbol{u}})\phi(t)dt$$

$$\Theta\left(\hat{\boldsymbol{U}}_k^T\right) = \left[1 \quad \hat{\boldsymbol{U}}_k^T \quad \hat{\boldsymbol{U}}_{k,P_2}^T \quad \ldots \quad \hat{\boldsymbol{U}}_{k,P_\ell}^T \quad \ldots \quad \sin(\hat{\boldsymbol{U}}_k^T) \quad \cos(\hat{\boldsymbol{U}}_k^T) \quad \ldots \quad \exp(\hat{\boldsymbol{U}}_k^T)\right]$$

*Messenger, Bortz. ”Weak SINDy: Galerkin-based data-driven model selection." Multiscale Modeling & Simulation, 19(3):1474-1497 (2021)

WgLaSDI: 2D Burger's Equation

Interpretable

- Autoencoder: 7200-100-5
- Basis functions: 2nd-order polynomials
- Noisy data: 10% noise
- 1 testing case

True solution - u component

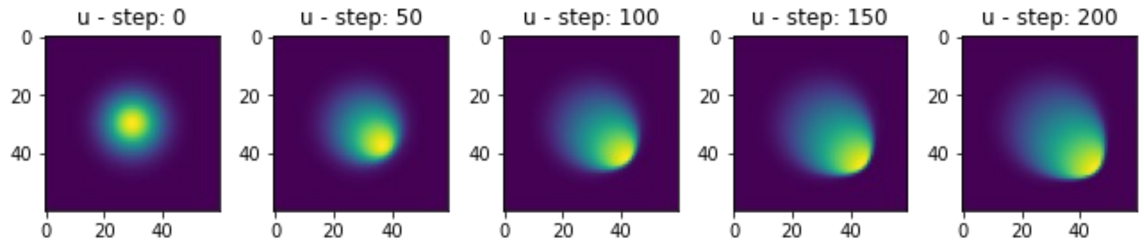

gLaSDI Max Relative Error: 1220.4%

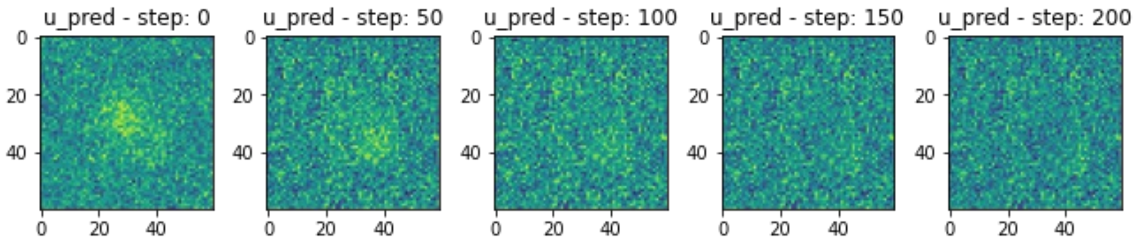

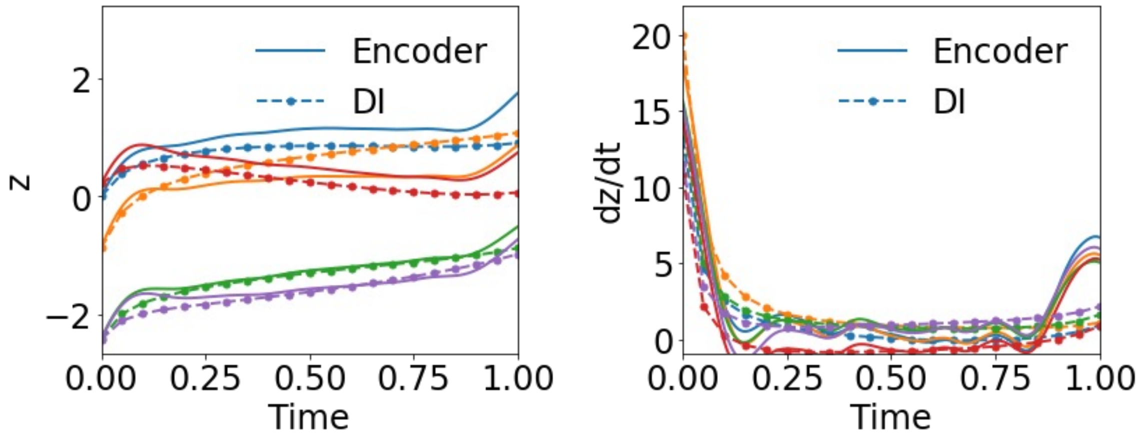

WgLaSDI Max Relative Error: 3.8%

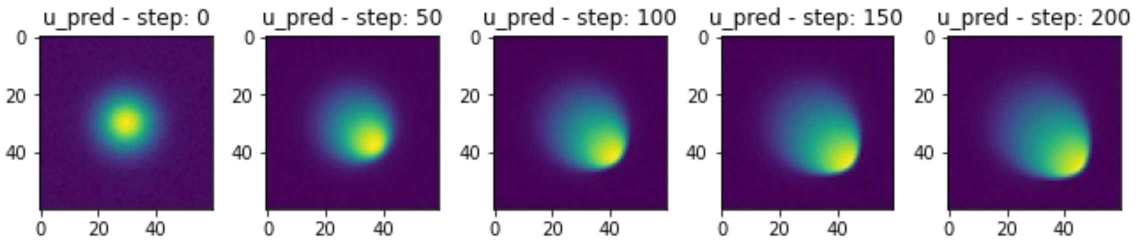

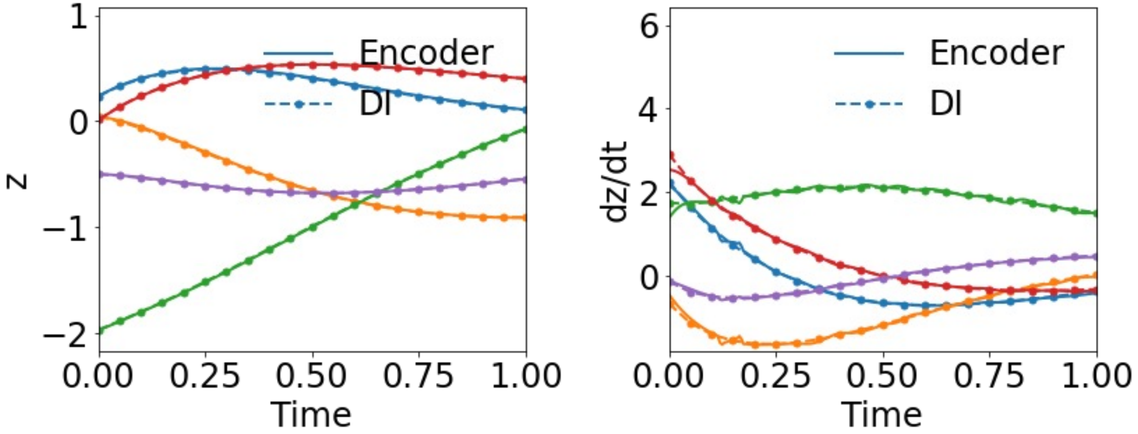

Interpretable

WgLaSDI: 2D Burger's Equation

- Parameter space: 441 cases (21x21)
- Noisy data: 10% noise

Autoencoder: 7200-100-**5**, Number of DIs: 36
Basis functions: 2nd-order polynomials
KNN (1) Greedy, KNN (4) Evaluation

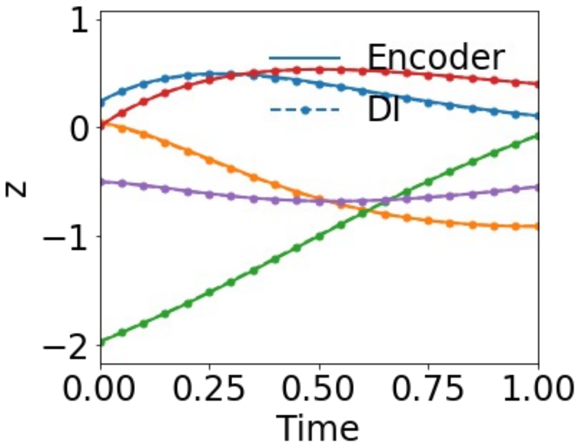

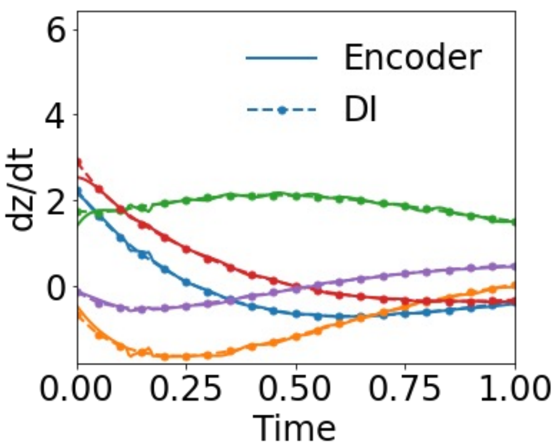

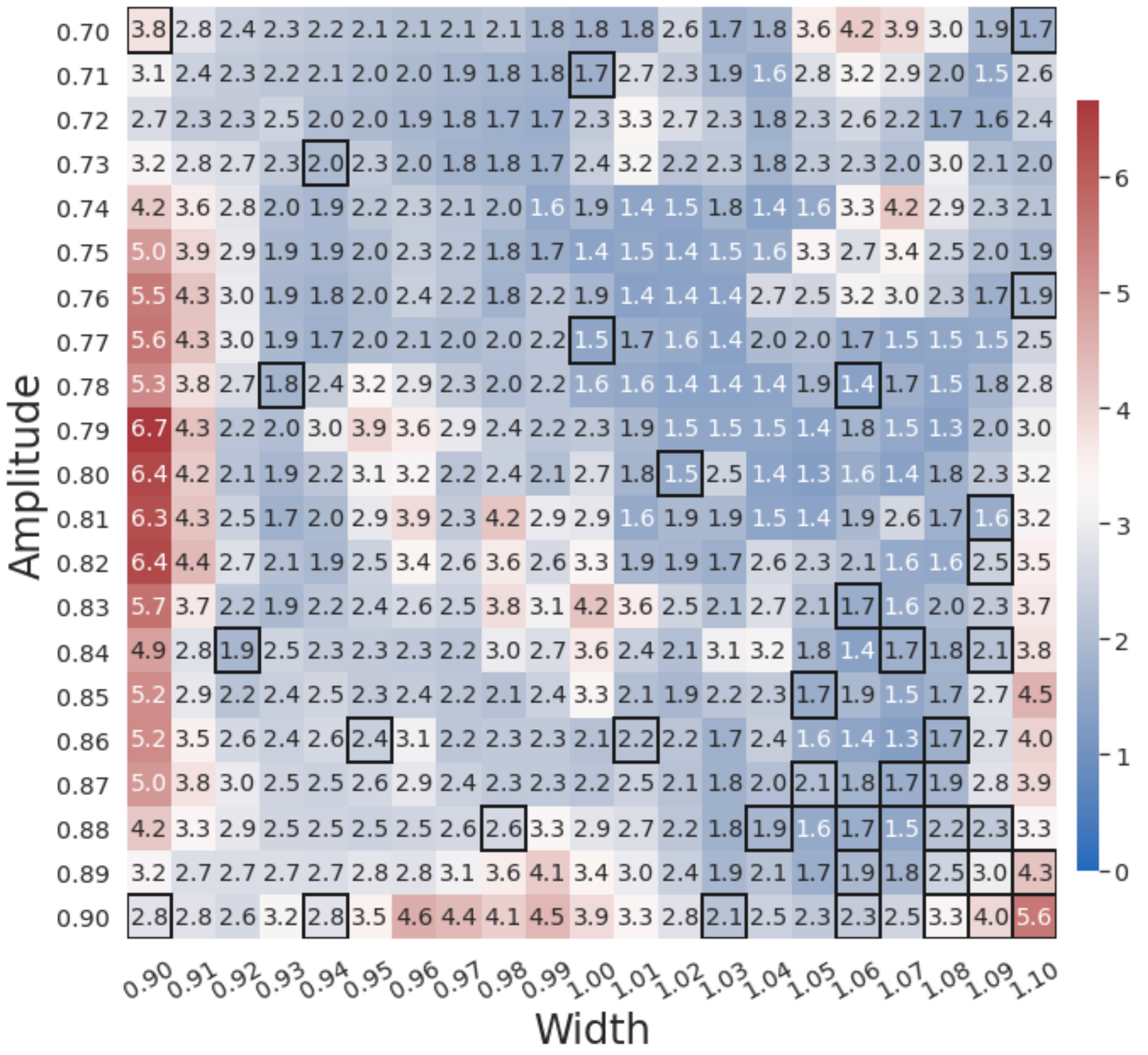

Addressing issue of **structure-preserving prediction**

Projection-based ROM


D. Copeland


S.W. Cheung

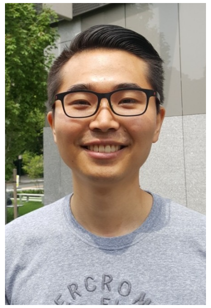
Y. Shin


J. Lauzon


K. Huynh

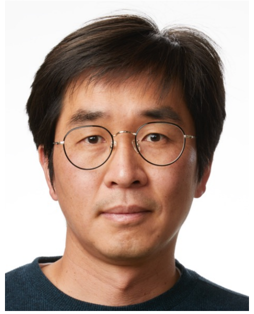
Y. Choi

How about physics-constrained model?

Latent space dynamics data
with a dimension of 3

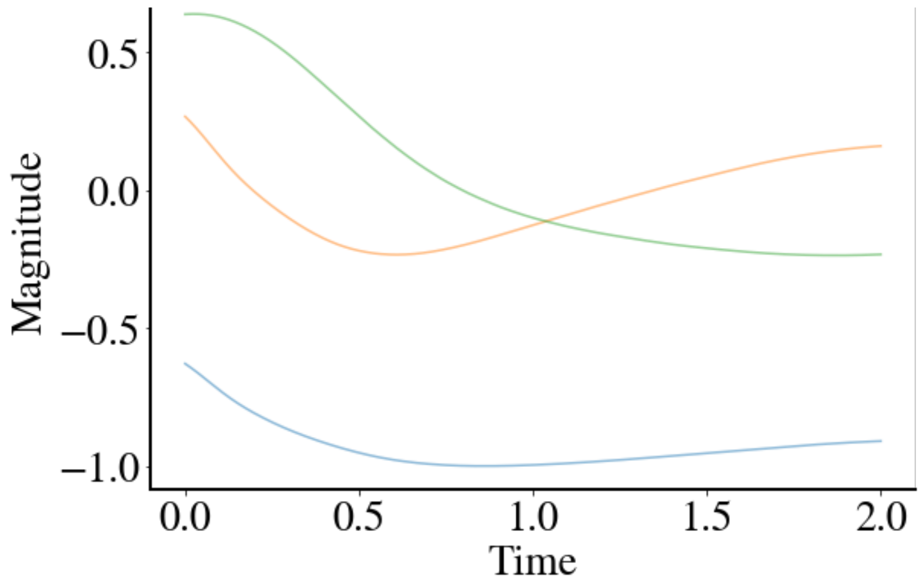

Derive ODEs from original governing equation?

Projection-based reduced order model

$$\frac{d\hat{\boldsymbol{u}}}{dt} = \hat{\boldsymbol{f}}(\hat{\boldsymbol{u}}; \boldsymbol{\mu})$$

Projection-based linear subspace reduced order model

- Governing equation: $\dfrac{d\boldsymbol{w}}{dt} = \boldsymbol{f}(\boldsymbol{w}, t; \boldsymbol{\mu}), \quad \boldsymbol{w}, \boldsymbol{f} \in \mathbb{R}^{N_s}$
- Solution approximation:

$$\boldsymbol{w} \approx \tilde{\boldsymbol{w}} = \boldsymbol{w}_{\text{ref}} + \boldsymbol{\Phi}\hat{\boldsymbol{w}}, \quad \boldsymbol{\Phi} \in \mathbb{R}^{N_s \times n_s}, \quad n_s \ll N_s$$

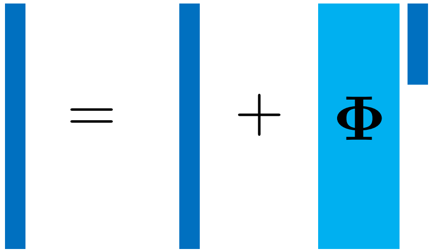

ODE for latent space dynamics derived completely from original governing equation!

- Reduced system after Galerkin projection: $\dfrac{d\hat{\boldsymbol{w}}}{dt} = \boldsymbol{\Phi}^T \boldsymbol{f}(\boldsymbol{w}_{\text{ref}} + \boldsymbol{\Phi}\hat{\boldsymbol{w}}, t; \boldsymbol{\mu})$
- Backward Euler time integrator: $\hat{\boldsymbol{w}}_n = \hat{\boldsymbol{w}}_{n-1} + \Delta t \boldsymbol{\Phi}^T \boldsymbol{f}(\boldsymbol{w}_{\text{ref}} + \boldsymbol{\Phi}\hat{\boldsymbol{w}}, t; \boldsymbol{\mu})$

Scales with FOM size: $\mathbb{R}^{N_s}$

Hyper-reduction: a point selection-based*

- Approximate nonlinear term:

$$\boldsymbol{f} \approx \boldsymbol{\Phi}_f \hat{\boldsymbol{f}}, \quad \boldsymbol{\Phi}_f \in \mathbb{R}^{N_s \times n_f}, \quad n_s \leq n_f \ll N_s$$

- Interpolation:

$$\boldsymbol{Z}^T \boldsymbol{f} = \boldsymbol{Z}^T \boldsymbol{\Phi}_f \hat{\boldsymbol{f}} \rightarrow \quad \hat{\boldsymbol{f}} = (\boldsymbol{Z}^T \boldsymbol{\Phi}_f)^{-1} \boldsymbol{Z}^T \boldsymbol{f}$$

sampling matrix, $\boldsymbol{Z} \in \mathbb{R}^{N_s \times n_f}$

- row pivoted LU decomposition: DEIM[1]
- column pivoted QR decomposition: Q-DEIM[2]
- column orthogonality & determinant: S-OPT[3]

- Replace nonlinear term:

$$\hat{\boldsymbol{w}}_n = \hat{\boldsymbol{w}}_{n-1} + \Delta t \boldsymbol{\Phi}^T \boldsymbol{\Phi}_f (\boldsymbol{Z}^T \boldsymbol{\Phi}_f)^{-1} \boldsymbol{Z}^T \boldsymbol{f}(\boldsymbol{w}_{\text{ref}} + \boldsymbol{\Phi} \hat{\boldsymbol{w}}, t; \boldsymbol{\mu})$$

😀 precompute

😀 work with only sampled rows

1. Chaturantabut, Sorensen. Nonlinear model reduction via discrete empirical interpolation. SISC, 32(5):2737–2764, 2010.
2. Drmac, Gugercin. A new selection operator for the discrete empirical interpolation method---improved a priori error bound and extensions. SISC, A631-A648, 2016.
3. Lauzon, Cheung, Shin, Choi, Copeland, Huynh. S-OPT: A point selection algorithm for hyper-reduction in reduced order models, arXiv:2203.16494, 2022

Physics-constrained

Improved hyper-reduction technique in physics-constrained data-driven reduced order models

S-OPT: stabilized point selection algorithm

Maximize **the column orthogonality** and **determinant** to resolve the unstable behavior of the classical DEIM approach.

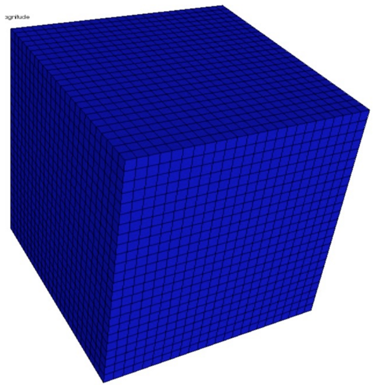

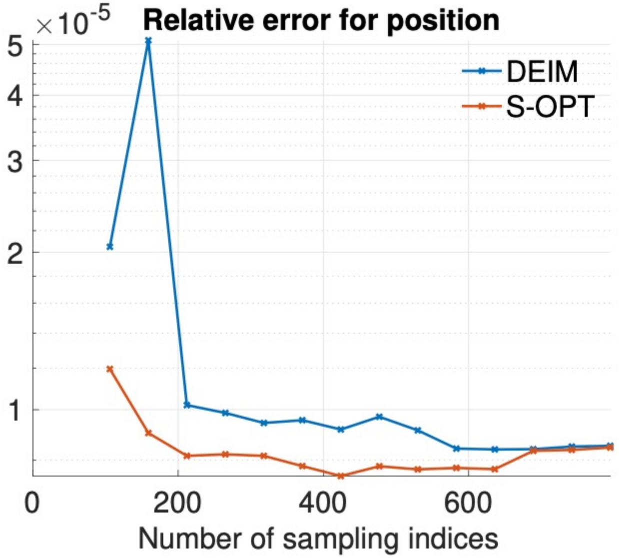

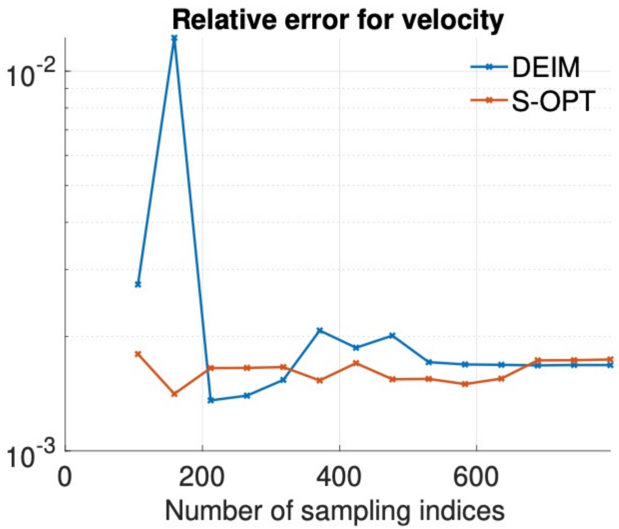

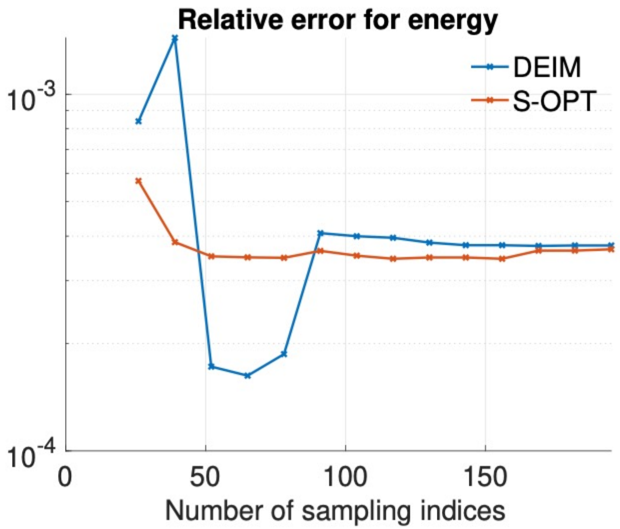

Publications:

- Lauzon, Cheung, Shin, Choi, Copeland, Huynh, "**S-OPT**: A points selection algorithm for hyper-reduction in reduced order models" arXiv:2203.16494 (submitted to SISC)

+ More stable behavior is achieved by S-OPT on Sedov blast hydrodynamics simulation than traditional DEIM approach!

Successful applications of linear subspace ROM

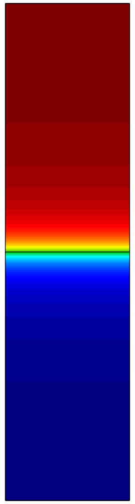

Rayleigh–Taylor
Kinematic dofs: 8,514
Energy dofs: 4,096
Wall-clock time: 127 sec

Relative error & speedup

Velocity: 7.8e-3
Speedup: 14.6

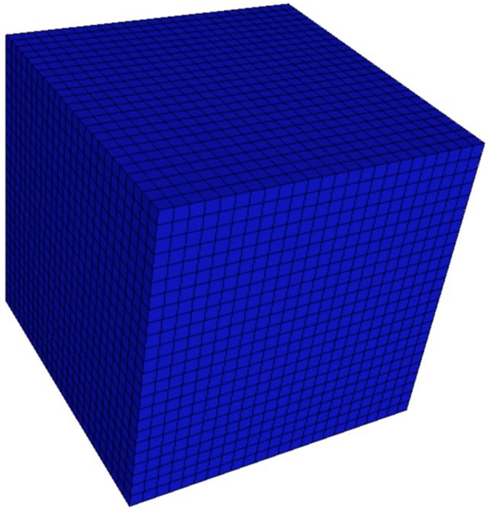

Sedov blast
Kinematic dofs: 14,739
Energy dofs: 4,096
Wall-clock time: 191 sec

Relative error & speedup

Velocity: 2.2e-4
Speedup: 22.8

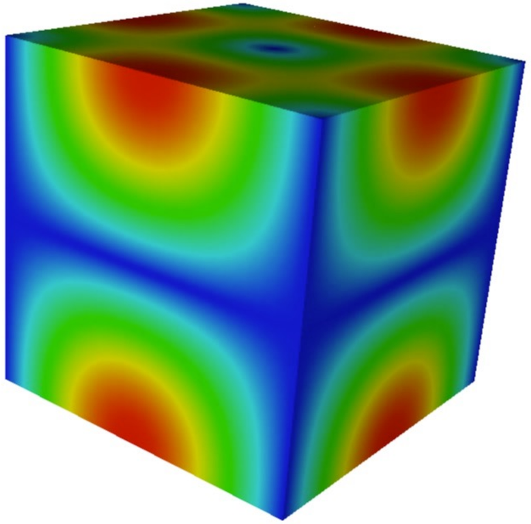

Taylor–Green
Kinematic dofs: 14,739
Energy dofs: 4,096
Wall-clock time: 170 sec

Relative error & speedup

Velocity: 1.1e-6
Speedup: 31.2

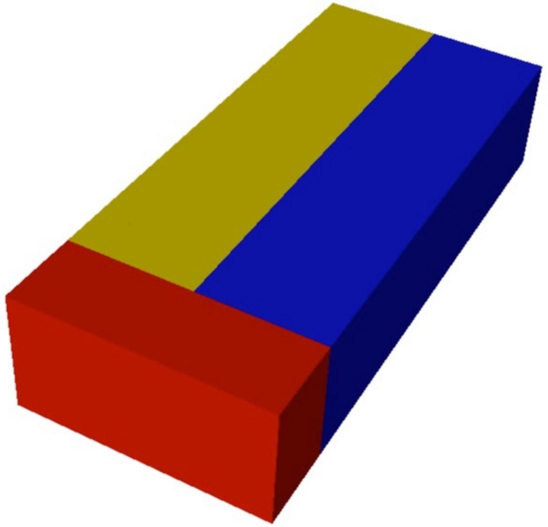

Triple-point problem
Kinematic dofs: 38,475
Energy dofs: 10,752
Wall-clock time: 122 sec

Relative error & speedup

Velocity: 8.1e-4
Speedup: 87.8

1. Copeland, Cheung, Huynh, Choi. Reduced order models for Lagrangian hydrodynamics, *CMAME*, 2022
2. Cheung, Choi, Copeland, Huynh. Local Lagrangian reduced-order modeling for the Rayleigh–Taylor instability by solution manifold decomposition, JCP, 2023

Physics-constrained ROM improves extrapolation accuracy

Extrapolation accuracy

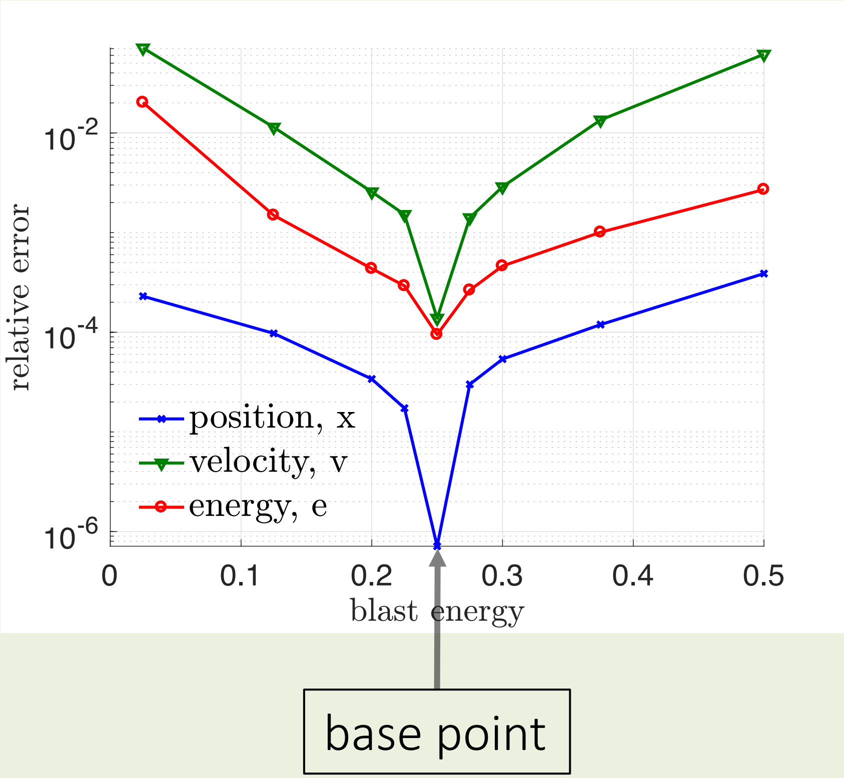

EC-EQP: Energy conserving empirical quadrature procedure

Run	S1A	S2A	S1B	S2B	S1C	S2C
Problem	Sedov	Sedov	Gresho	Gresho	TG	TG
t_f	0.01	0.05	0.01	0.02	0.01	0.02
T_s	1	5	1/2	1	1	2
$\epsilon_{x,B}$	6.43e-06	3.90e-04	8.24e-06	5.02e-05	3.13e-06	1.58e-04
$\epsilon_{v,B}$	1.21e-02	8.90e-02	3.99e-03	1.10e-02	1.86e-03	3.43e-02
$\epsilon_{e,B}$	1.51e-02	6.36e-03	2.38e-03	1.66e-03	5.86e-05	2.13e-03
ΔE_B	3.74e-02	7.80e-05	5.50e-05	7.82e-05	8.05e-07	3.64e-06
S_B	2.26	2.04	2.62	2.63	2.17	2.21
$\epsilon_{x,EC}$	2.02e-05	3.49e-05	1.27e-05	1.90e-04	8.31e-05	1.14e-03
$\epsilon_{v,EC}$	7.77e-03	7.02e-03	8.44e-03	1.21e-01	3.60e-02	2.79e-01
$\epsilon_{e,EC}$	1.23e-03	7.77e-04	3.68e-03	1.41e-02	1.63e-03	9.58e-03
ΔE_{EC}	1.31e-14	2.73e-13	2.40e-12	6.53e-12	2.66e-11	1.13e-10
S_{EC}	2.25	1.89	2.50	2.10	2.11	2.18

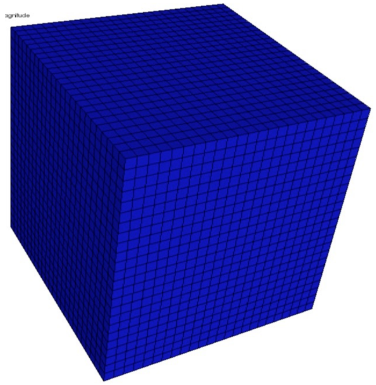

Report:

- Vales, Choi, Copeland, Cheung, "Energy conserving quadrature based dimensionality reduction for nonlinear hydrodynamics problems" LLNL-TR-853055

Component-wise ROM


S. Chung

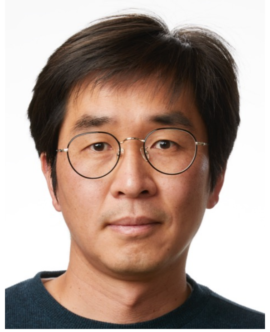
Y. Choi


P. Roy


T. Moore


T. Roy


S. Baker


T. Lin


E. Duoss


C. Hahn

Homogeneous Neumann boundary

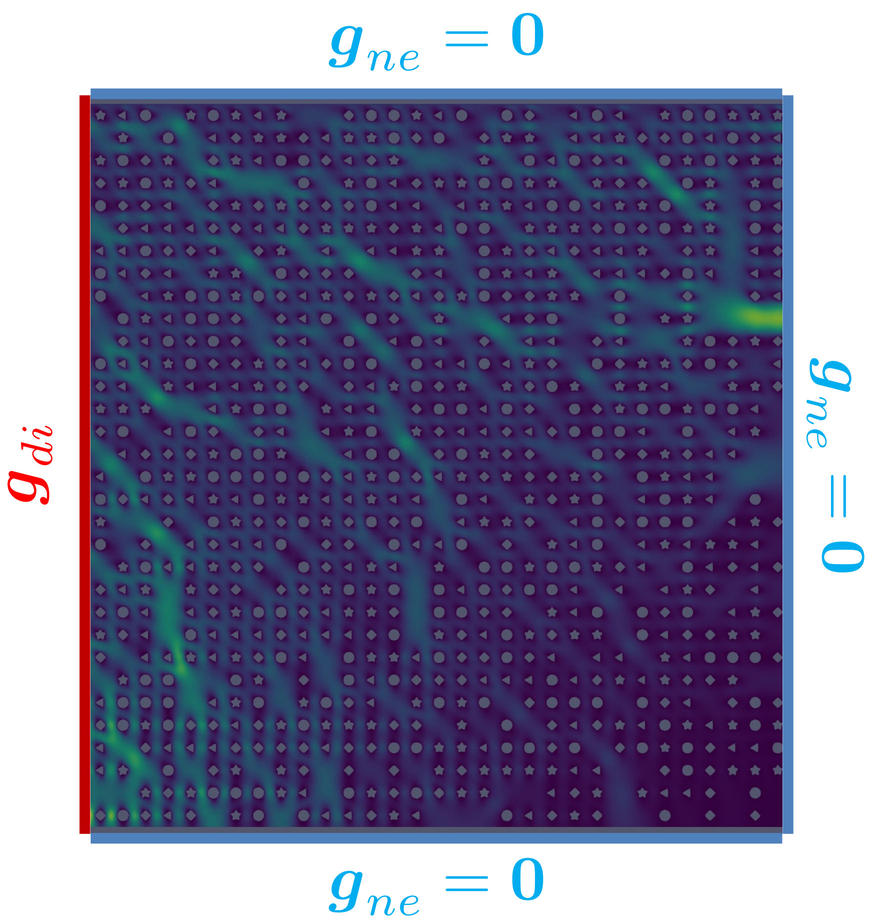

Channel flow

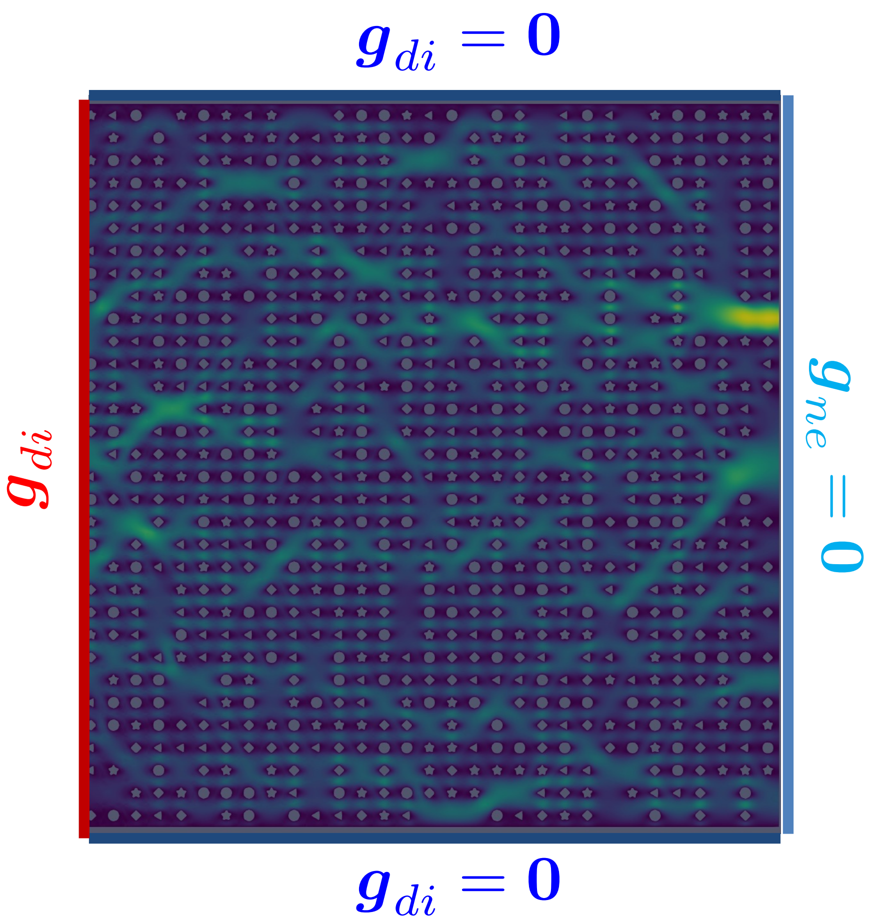

Stokes equations

$$-\nu\nabla^2\tilde{\boldsymbol{u}} + \nabla\tilde{p} = 0 \quad \text{in } \Omega$$

$$\nabla\cdot\tilde{\boldsymbol{u}} = 0 \quad \text{in } \Omega$$

$$\tilde{\boldsymbol{u}} = \boldsymbol{g}_{di} \quad \text{on } \partial\Omega_{di}$$

$$\boldsymbol{n}\cdot(-\nu\nabla\tilde{\boldsymbol{u}} + \tilde{p}\boldsymbol{I}) = \boldsymbol{g}_{ne} \quad \text{on } \partial\Omega_{ne}$$

Reference components

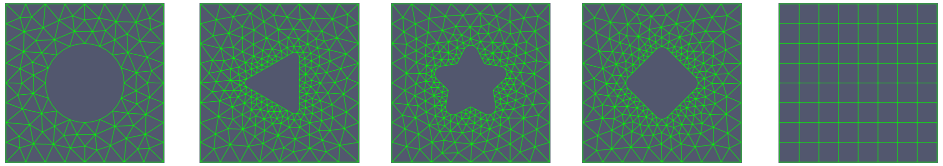

Training

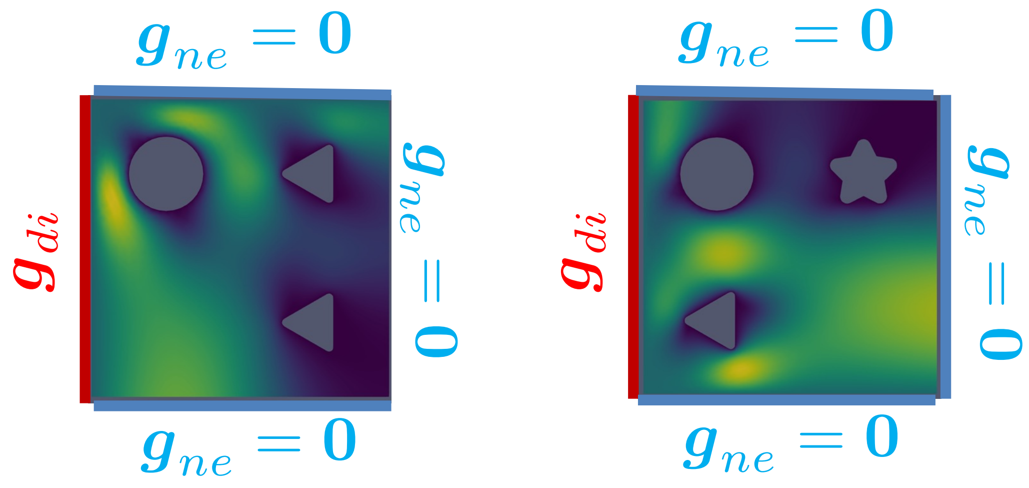

Inflow condition

$$\boldsymbol{g}_{di} = (g_1 + \Delta g_1 \sin 2\pi(\mathbf{k}_1\cdot\boldsymbol{x} + \theta_1), g_2 + \Delta g_2 \sin 2\pi(\mathbf{k}_2\cdot\boldsymbol{x} + \theta_2))$$

Homogeneous Neumann boundary

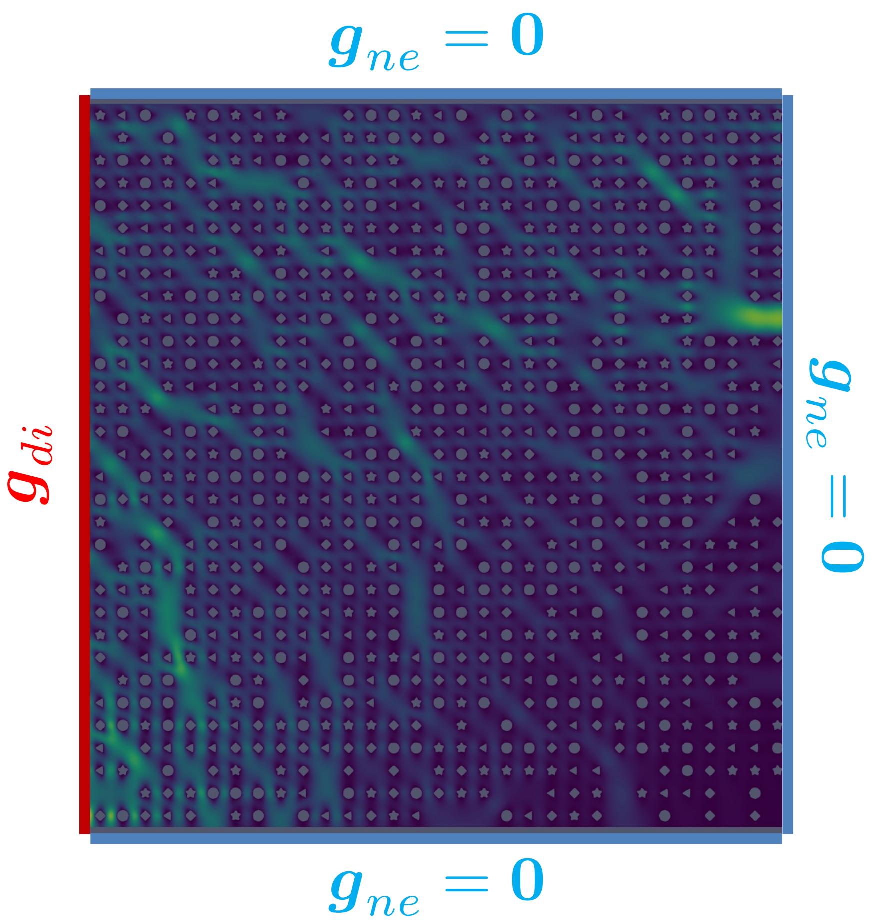

Channel flow

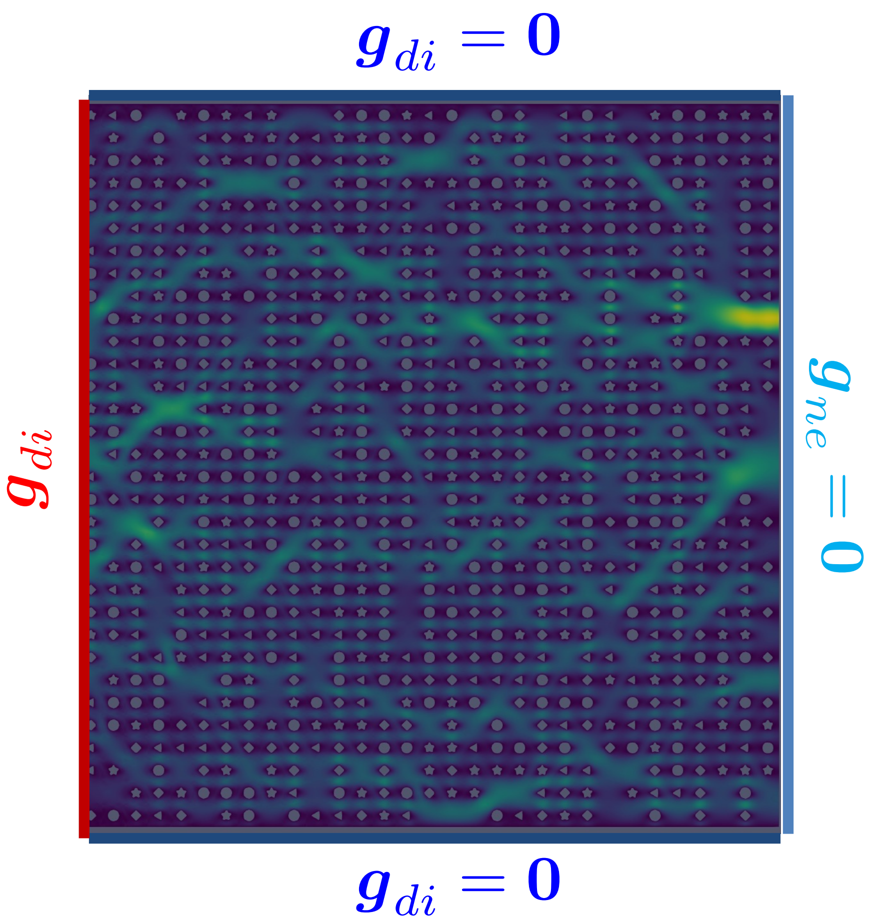

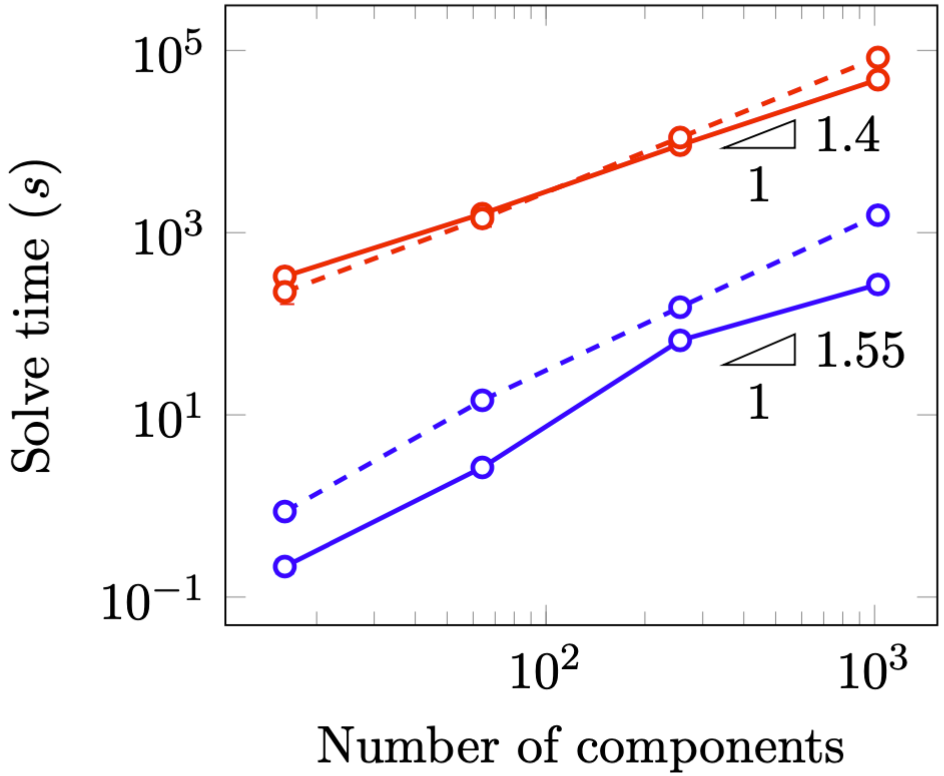
Solve time (s)
10^5
10^3
10^1
10^{-1}
1.4
1
1.55
1
10^2
10^3
Number of components

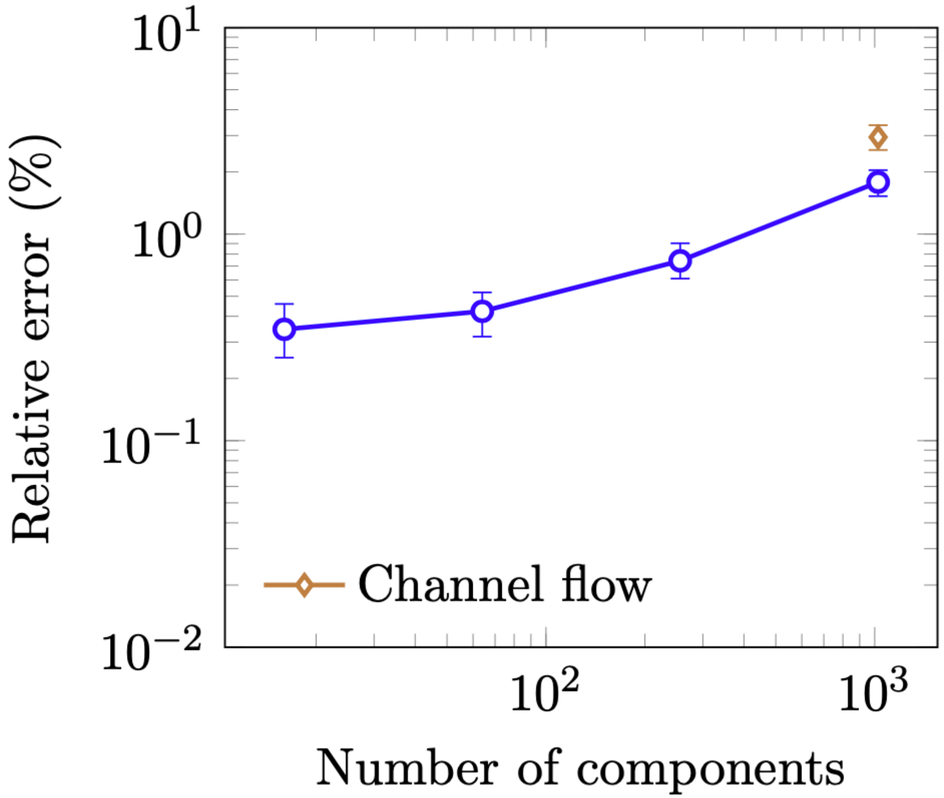
Relative error (%)
10^1
10^0
10^{-1}
10^{-2}
Channel flow
10^2
10^3
Number of components

Nonlinear manifold ROM

Y. Kim

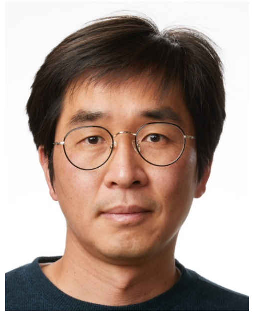

Y. Choi

D. Widemann

T. Zohdi

FOM

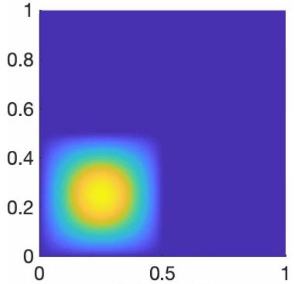

- Governing equation:

$$\frac{d\boldsymbol{w}}{dt} = \boldsymbol{f}(\boldsymbol{w}, t; \boldsymbol{\mu}) \quad \boldsymbol{w}, \boldsymbol{f} \in \mathbb{R}^{N_s}$$

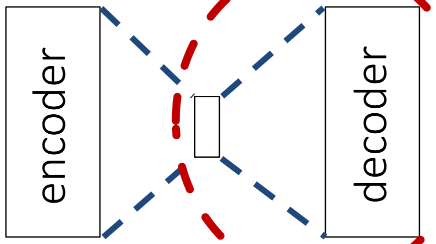

linear subspace PROM

- Solution approximation:

$$\boldsymbol{w} \approx \tilde{\boldsymbol{w}} = \boldsymbol{w}_{\text{ref}} + \boldsymbol{\Phi}\hat{\boldsymbol{w}},$$

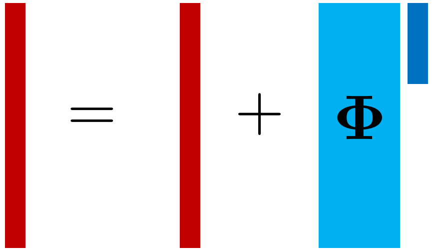

$$\boldsymbol{\Phi} \in \mathbb{R}^{N_s \times n_s}, \quad n_s \ll N_s$$

- Reduced system after Galerkin projection:

$$\frac{d\hat{\boldsymbol{w}}}{dt} = \boldsymbol{\Phi}^T \boldsymbol{f}(\boldsymbol{w}_{\text{ref}} + \boldsymbol{\Phi}\hat{\boldsymbol{w}}, t; \boldsymbol{\mu})$$

LS-PROM

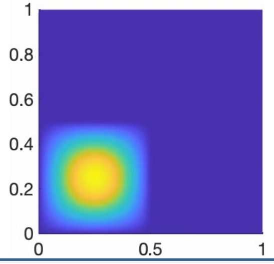

Low rank of **5**
Max. rel. error: **34.4%**
Speed-up: **26.8**

hyper-reduction

Nonlinear manifold PROM

- Solution approximation:

$$\boldsymbol{w} \approx \tilde{\boldsymbol{w}} = \boldsymbol{w}_{\text{ref}} + \boldsymbol{g}(\hat{\boldsymbol{w}}),$$

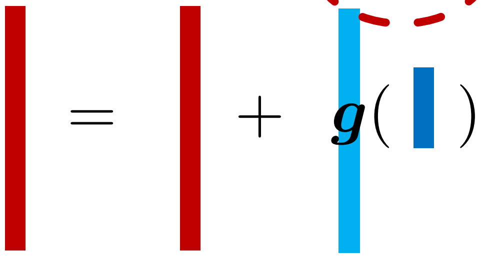

$$\hat{\boldsymbol{w}} \in \mathbb{R}^{n_s}, \quad n_s \ll N_s$$

- Reduced system after Galerkin projection:

$$\frac{d\hat{\boldsymbol{w}}}{dt} = \boldsymbol{J}_g(\hat{\boldsymbol{w}})^\dagger \boldsymbol{f}(\boldsymbol{w}_{ref} + \boldsymbol{g}(\hat{\boldsymbol{w}}), t; \boldsymbol{\mu})$$

NM-PROM

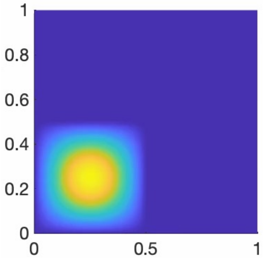

Low rank of **5**
Max. rel. error: **0.93%**
Speed-up: **11.6**

Shallow vs. deep NN in the perspective of hyper-reduction

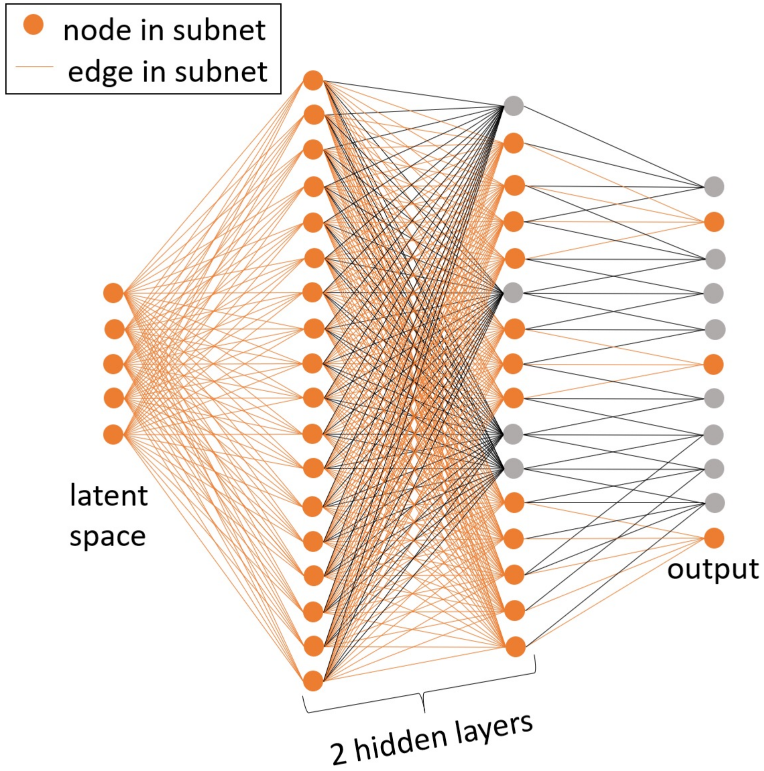

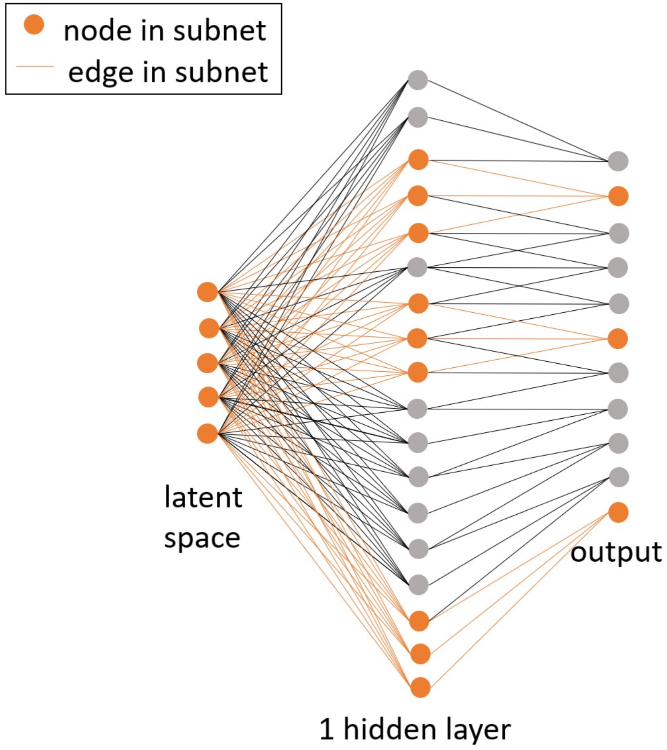

- A shallow neural network can provide sparser structure than a deep one in a subnet
- A sparse network is a key for successful NM-ROM hyper-reduction!

*Kim, Choi, Widemann, and Zohdi, "A fast and accurate physics-informed neural network reduced order model with shallow masked autoencoder." Journal of Computational Physics, 110841, 2021.

Domain decomposition NM-ROM


A. Diaz

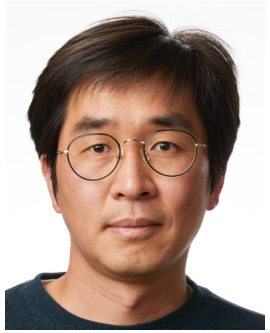
Y. Choi


M. Heinkenschloss

Domain-decomposition nonlinear manifold ROMs

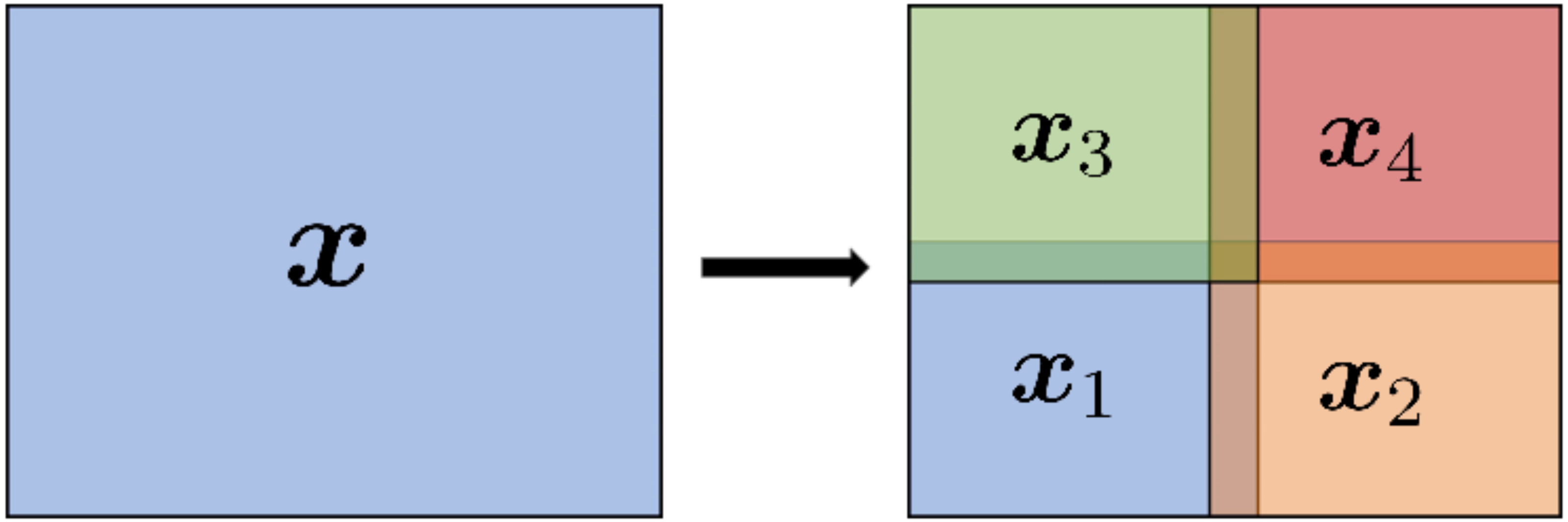

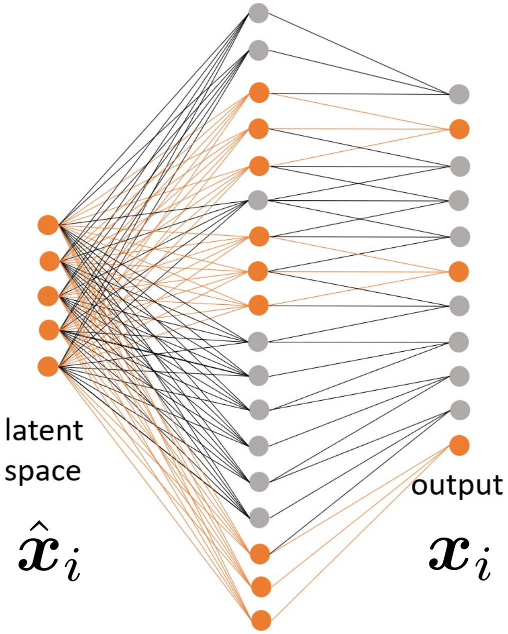

$$\boldsymbol{x}_i \approx \boldsymbol{g}_i(\hat{\boldsymbol{x}}_i)$$

*Diaz, Choi, Heinkenschloss, “A fast and accurate domain-decomposition nonlinear manifold reduced order model." *arXiv preprint*, arXiv:2305.15163, 2023.

DD NM-ROM

- Compute decoder $\boldsymbol{g}_i : \mathbb{R}^{n_i} \to \mathbb{R}^{N_i}$ for each subdomain
- Solve minimization problem to evaluate DD NM-ROM

$$\min_{\widehat{\boldsymbol{x}}_i} \frac{1}{2} \sum_{i=1}^{4} \|\boldsymbol{B}_i \boldsymbol{r}_i(\boldsymbol{g}_i(\widehat{\boldsymbol{x}}_i); \boldsymbol{\mu})\|_2^2 \quad \text{s.t.} \quad \sum_{i=1}^{4} \boldsymbol{C}\boldsymbol{A}_i \boldsymbol{g}_i(\widehat{\boldsymbol{x}}_i) = \boldsymbol{0}$$

- $\boldsymbol{B}_i$ sampling matrix for hyper reduction
- $\boldsymbol{C}$ “test matrix” to avoid overdetermined problem
- Solve using inexact Lagrange-Newton SQP solver

DD-NMROM achieves a great accuracy on 2D steady state Burgers' EQ

$$v_1 \frac{\partial v_1}{\partial x} + v_2 \frac{\partial v_1}{\partial y} = \nu \left(\frac{\partial^2 v_1}{\partial x^2} + \frac{\partial^2 v_1}{\partial y^2} \right) \qquad v_1 \frac{\partial v_2}{\partial x} + v_2 \frac{\partial v_2}{\partial y} = \nu \left(\frac{\partial^2 v_2}{\partial x^2} + \frac{\partial^2 v_2}{\partial y^2} \right)$$

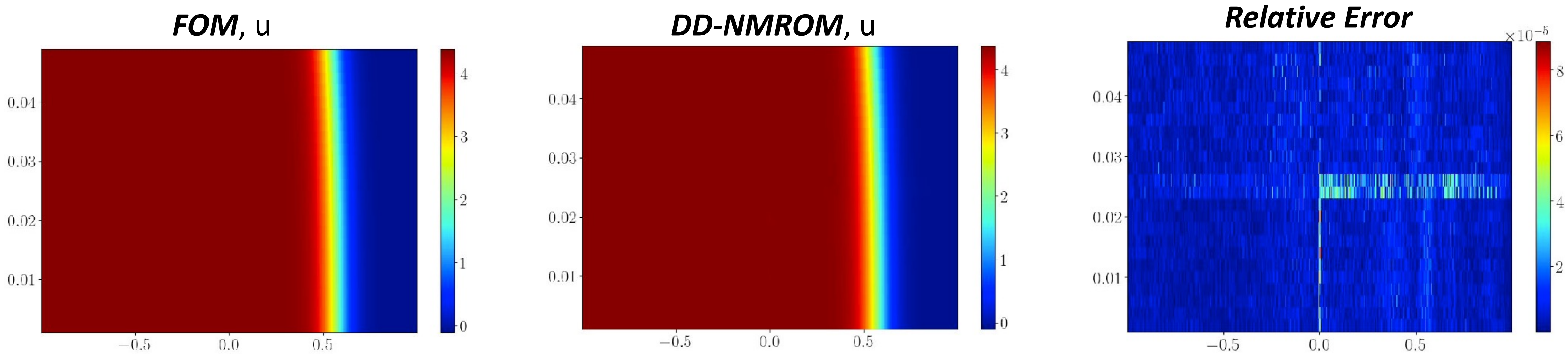

ROM DoF (aggregated)	% Dimension Reduction	Relative Error	Online Speedup
48	0.19%	1.64×10^{-3}	43.9

Summary and conclusion

- **Four different issues of** data-driven approaches:
  - Relying on big data -> curse of dimensionality
  - Interpretability
  - Not structure-preserving prediction
  - Not robust in extrapolation

- **Examples**:
  - **LaSDI**: Latent space dynamics identification

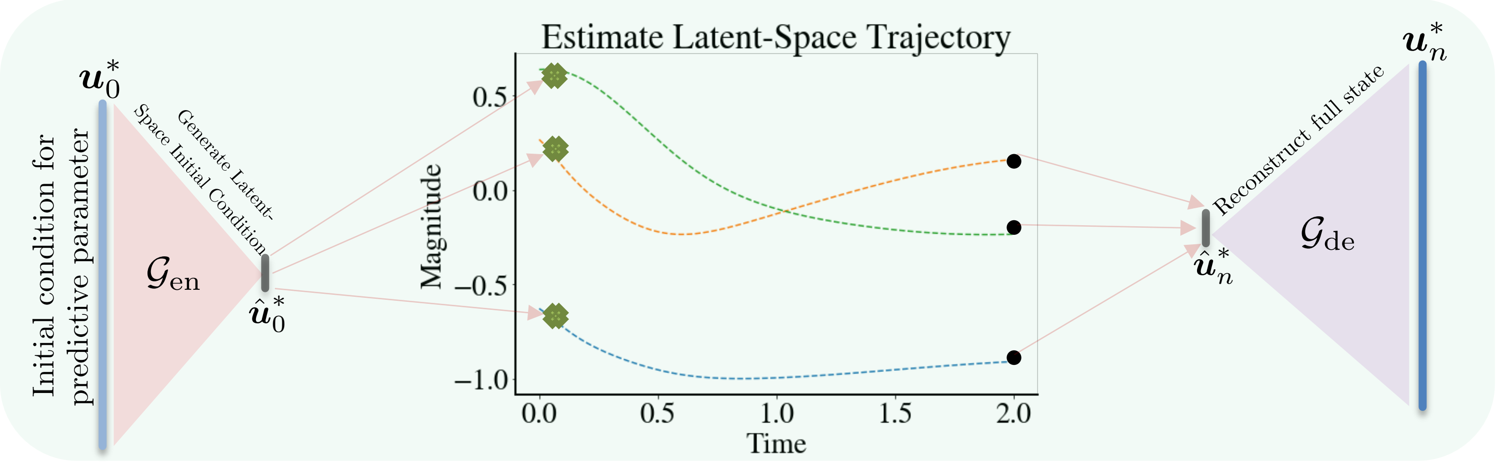

Summary and conclusion

- **Four different issues of** data-driven approaches:
  - — Relying on big data -> curse of dimensionality
  - — Interpretability
  - — Not structure-preserving prediction
  - — Not robust in extrapolation

- **Examples**:
  - — **LaSDI**: Latent space dynamics identification
  - — **Greedy sampling:**
    - • Physics-informed

Uniform sampling

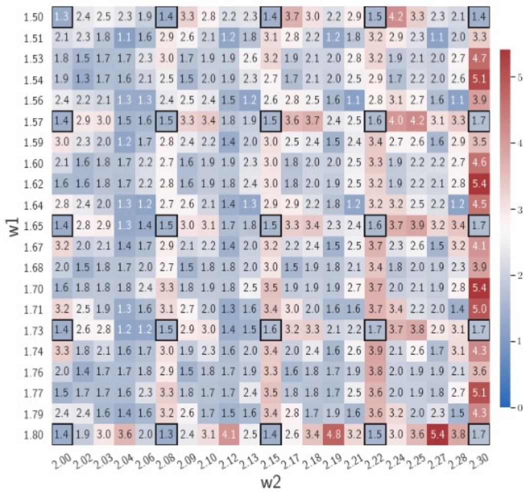

Physics-informed

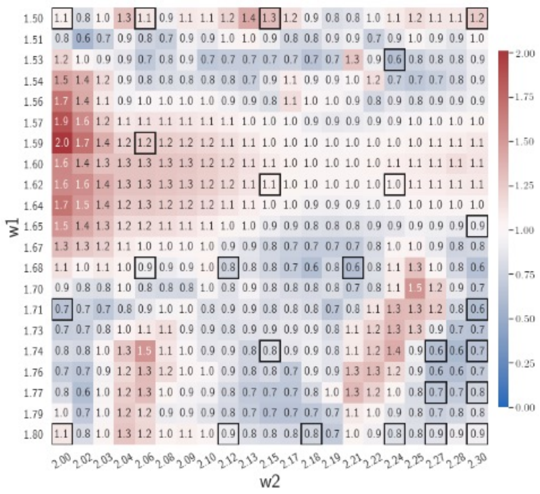

Summary and conclusion

- **Four different issues of** data-driven approaches:
  - — Relying on big data -> curse of dimensionality
  - — Interpretability
  - — Not structure-preserving prediction
  - — Not robust in extrapolation

- **Examples**:
  - — **LaSDI**: Latent space dynamics identification
  - — **Greedy sampling:**
    - Physics-informed
    - uncertainty-guided

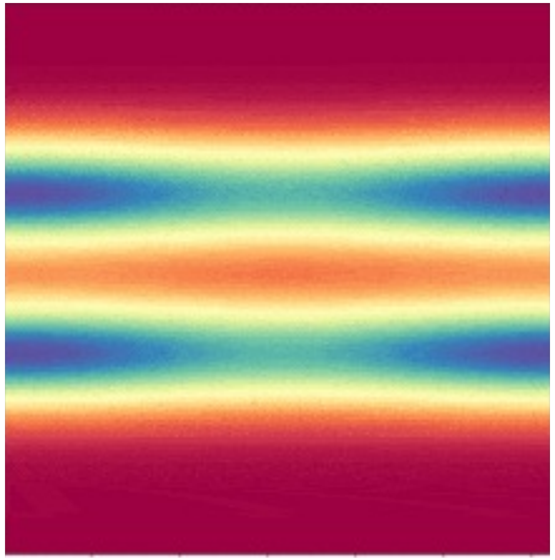

Summary and conclusion

- **Four different issues of** data-driven approaches:
  - — Relying on big data -> curse of dimensionality
  - — Interpretability
  - — Not structure-preserving prediction
  - — Not robust in extrapolation

- **Examples**:
  - — **LaSDI**: Latent space dynamics identificatiom
  - — **Greedy sampling:**
    - Physics-informed
    - uncertainty-guided
  - — **DMD**: Dynamic mode decomposition

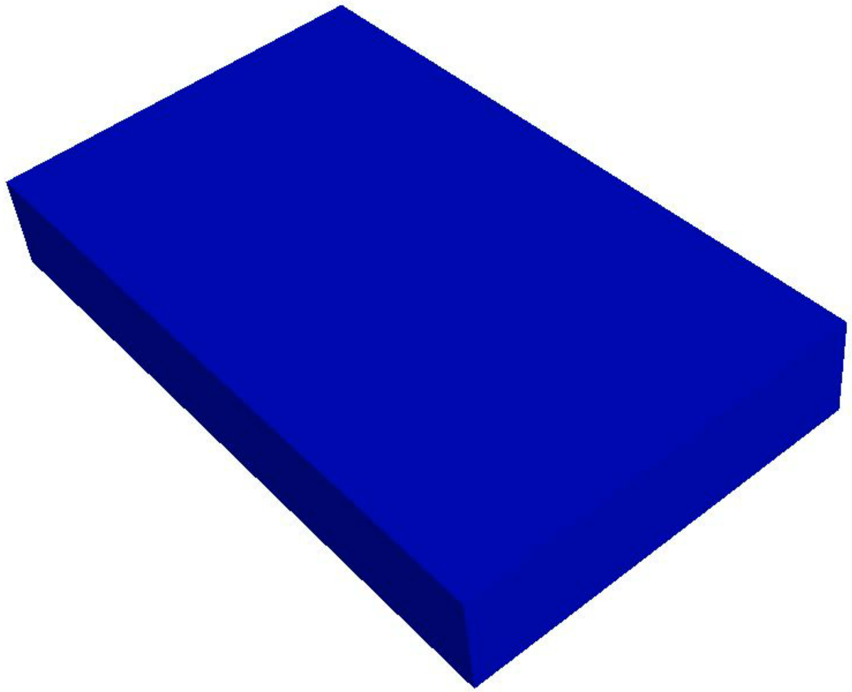

Summary and conclusion

- **Four different issues of** data-driven approaches:
  - — Relying on big data -> curse of dimensionality
  - — Interpretability
  - — Not structure-preserving prediction
  - — Not robust in extrapolation

- **Examples**:
  - — **LaSDI**: Latent space dynamics identification
  - — **Greedy sampling:**
    - Physics-informed
    - uncertainty-guided
  - — **DMD**: Dynamic mode decomposition
  - — **WgLaSDI**: Weak gLaSDI

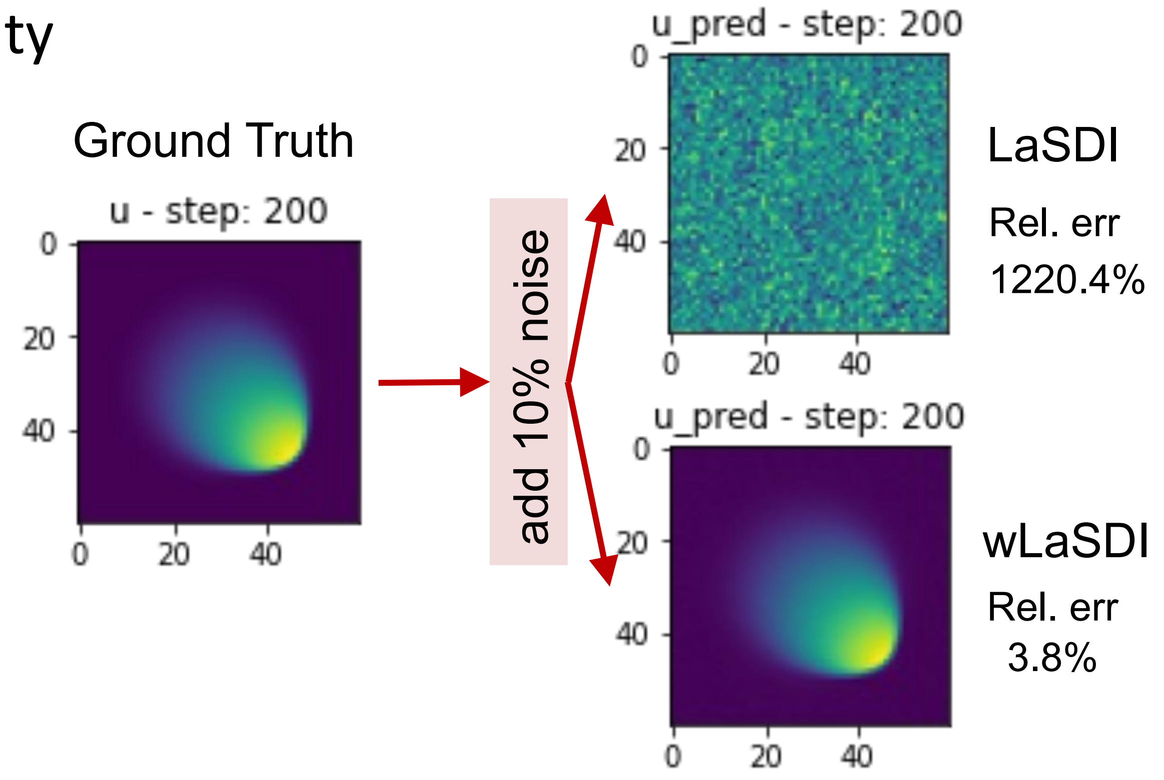

Summary and conclusion

- **Four different issues of** data-driven approaches:
  - Relying on big data -> curse of dimensionality
  - Interpretability
  - Not structure-preserving prediction
  - Not robust in extrapolation

- **Examples**:
  - **LaSDI**: Latent space dynamics identification
  - **Greedy sampling:**
    - Physics-informed
    - uncertainty-guided
  - **DMD**: Dynamic mode decomposition
  - **WgLaSDI**: Weak gLaSDI
  - **pROM**: projection-based ROM

$$\boldsymbol{w} \approx \tilde{\boldsymbol{w}} = \boldsymbol{w}_{\mathrm{ref}} + \boldsymbol{\Phi}\hat{\boldsymbol{w}},$$

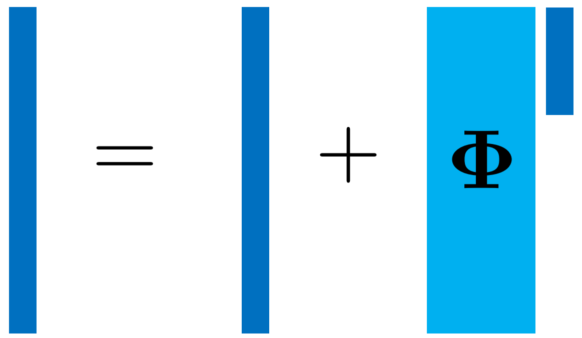

Summary and conclusion

- **Four different issues of** data-driven approaches:
  - Relying on big data -> curse of dimensionality
  - Interpretability
  - Not structure-preserving prediction
  - Not robust in extrapolation

- **Examples**:
  - **LaSDI**: Latent space dynamics identification
  - **Greedy sampling:**
    - Physics-informed
    - uncertainty-guided
  - **DMD**: Dynamic mode decomposition
  - **WgLaSDI**: Weak gLaSDI
  - **pROM**: projection-based ROM
  - **NM-ROM**: Nonlinear manifold ROM

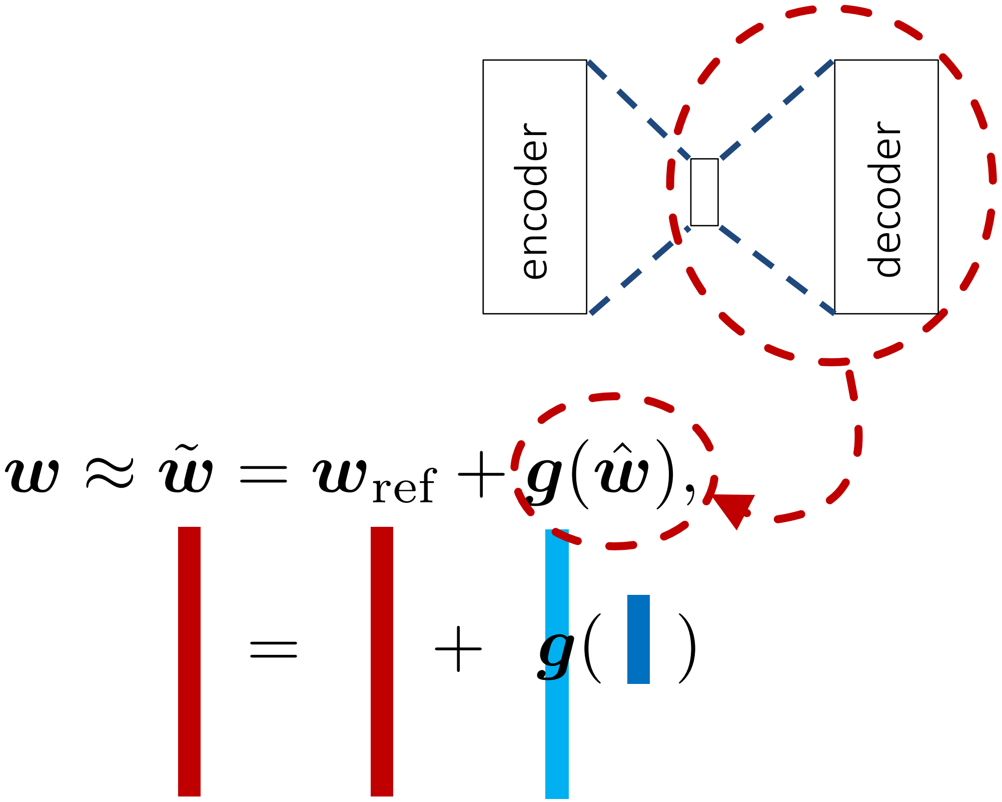

Summary and conclusion

- **Four different issues of** data-driven approaches:
  — Relying on big data -> curse of dimensionality
  — Interpretability
  — Not structure-preserving prediction
  — Not robust in extrapolation

- **Examples**:
  — **LaSDI**: Latent space dynamics identification
  — **Greedy sampling:**
    - Physics-informed
    - uncertainty-guided
  — **DMD**: Dynamic mode decomposition
  — **WgLaSDI**: Weak gLaSDI
  — **pROM**: projection-based ROM
  — **NM-ROM**: Nonlinear manifold ROM
  — **DD-NM-ROM**: Domain decomposition NM-ROM

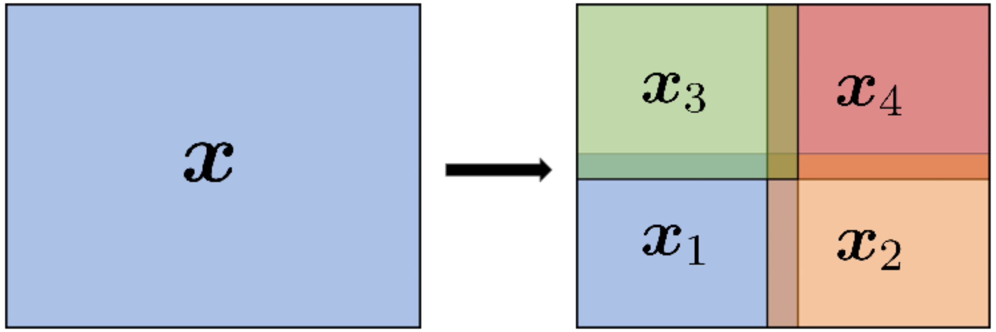

Questions? Email choi15@llnl.gov

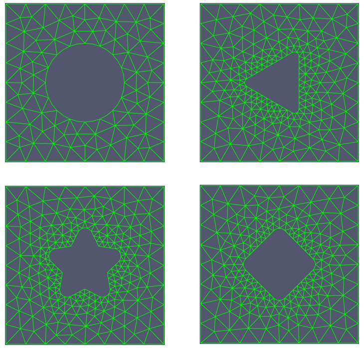

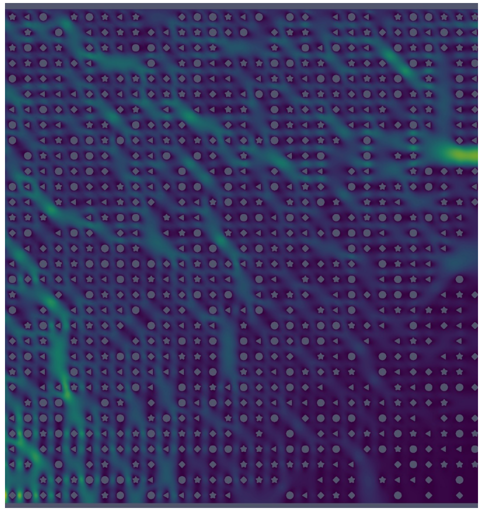

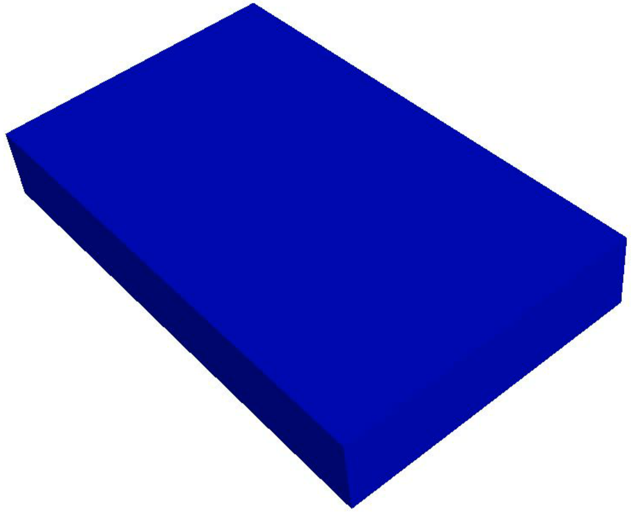

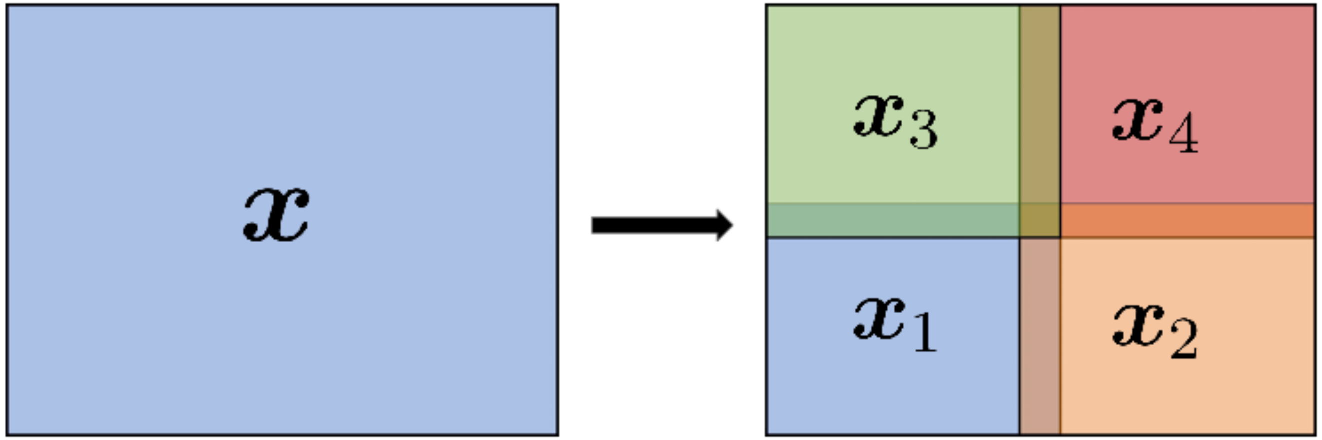

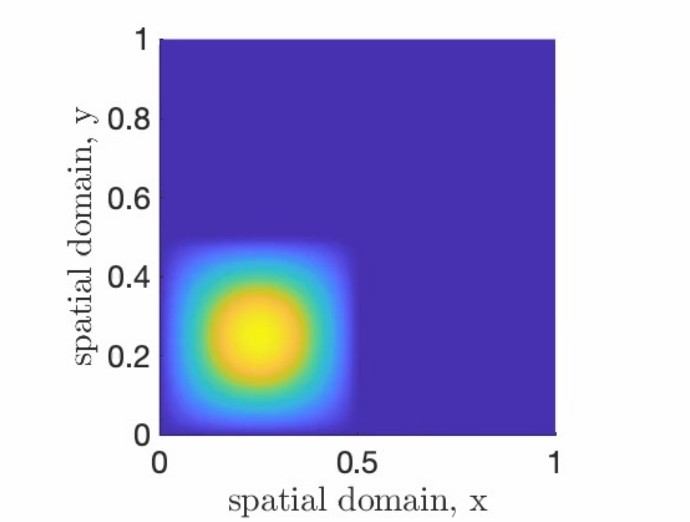

Lawrence Livermore National Laboratory